

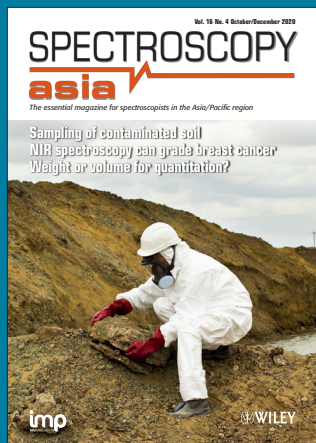
SPECTROSCOPY

asia

The essential magazine for spectroscopists in the Asia/Pacific region

Sampling of contaminated soil
NIR spectroscopy can grade breast cancer
Weight or volume for quantitation?





Representative sampling is always important, but when contamination is involved, it is particularly so. Find out more in the Sampling Column starting on page 22.

Publisher

Ian Michael
(ian@impublications.com)

Advertising Sales UK and Ireland

Ian Michael
Spectroscopy Asia, 6 Charlton Mill,
Charlton, Chichester, West Sussex PO18 0HY,
United Kingdom. Tel: +44-1243-811334,
Fax: +44-1243-811711,
E-mail: ian@impublications.com

Americas

Joe Tomaszewski
John Wiley & Sons Inc.
Tel: +1-908-514-0776
E: jtomaszewski@wiley.com

Europe and the Rest of World

Vanessa Winde
Wiley-VCH Verlag GmbH & Co. KGaA,
Boschstraße 12, 69469 Weinheim, Germany
Tel: +49 6201 606 721
E-mail: vanessa.winde@wiley.com

Circulation

Spectroscopy Asia Subscriptions, IM
Publications, 6 Charlton Mill, Charlton,
Chichester, West Sussex PO18 0HY UK.
E-mail: subs@impublications.com

Spectroscopy Asia is a joint publication of
John Wiley & Sons Ltd, The Atrium, Southern
Gate, Chichester, West Sussex PO19 8SQ, UK,
and IM Publications, 6 Charlton Mill, Charlton,
Chichester, West Sussex PO18 0HY, UK.

Vol. 16 No. 4
October/December 2020

2 SPECTROSCOPYASIA

ISSN 1743-5277

CONTENTS

3 Editorial

4 News

8 Study on lipid metabolism in human breast tissues by near infrared spectroscopy

Shuo He Yan, Zheng Zhu and Joëlle Wallon

14 Sponsored Article: Column properties that make an impact on ion chromatography

Carl Fisher and John Guajardo

19 Tony Davies Column: Weights or measures for better calibration

Antony N. Davies and Henk-Jan van Manen

22 Sampling Column: Chemical analysis of contaminated soil for sound environmental site assessment. Part 2

Jean-Sébastien Dubé and François Duhaime

28 New Products

Spectroscopy Asia is a controlled circulation journal, published four times a year and available free-of-charge to qualifying individuals in the Asia-Pacific region. Others can subscribe at the rate of €120 (Europe), £83 (UK), \$160 (ROW, postage included) for the four issues published in 2016. All paid subscription enquiries should be addressed to: *Spectroscopy Asia*, John Wiley & Sons Ltd, Journals Administration Department, The Atrium, Southern Gate, Chichester, West Sussex PO19 8SQ, UK.

Copyright 2020 John Wiley & Sons Ltd and IM Publications LLP

All rights reserved. No part of this publication may be reproduced, stored in a retrieval system, or transmitted, in any form or by any means, electronic, mechanical, photocopying, recording or otherwise, without the prior permission of the publisher in writing.
Printed in Singapore by C.O.S. Printers Pte Ltd.

WILEY

imp
impublications

A favour: let's keep in touch

With many people working remotely due to the coronavirus pandemic, it is a sensible time to ask you to check the details we hold for you regarding your free subscription to *Spectroscopy Asia*. In particular, it is important for successful communication that we have an up-to-date e-mail address.

Update your profile

Please go to <https://www.spectroscopyasia.com/user> and update your information by logging in and clicking on Edit Profile. (Your e-mail address will work as the username.) If you have forgotten your password, there is a link to Reset your Password. If you can't login, see the guide opposite.

Please check and update your details and when you get to the last page, you can select options as to how you wish to receive *Spectroscopy Asia* and how you wish us to communicate with you.

I cannot login

If you cannot login, you have two options:

- 1) Create a new account, and on the final page of the form tick the box that you already receive a print copy and enter your customer number from the label carrier (if you still have it). Here, you can also select options as to how you wish to receive *Spectroscopy Asia* and your communication preferences. We will then remove the old, duplicate account for you.
- 2) E-mail subs@impublications.com with your customer number and address details. We will locate your account, update your e-mail address and send you details so you can log in.

La Michael



14-16 January 2021 / Amsterdam, The Netherlands

If you are dealing with :

- spectroscopy
 - imaging spectroscopy
 - hyperspectral sensing
- the Spectro Expo is made for you !

The event will feature:

- 3 scientific conferences
- tutorials
- a commercial expo

Come and present your products, meet your future clients or future partners, learn about the latest developments in spectral sensing, from sensors design to advanced processing algorithms, for a variety of applications.

When: 14-16 January 2021,

Where: Amsterdam, The Netherlands



www.SpectroExpo.com - contact/info : adrianna.leroy@spectroexpo.com



Photo by Dylan de Jonge on Unsplash

SORS doesn't waste a drop

Iconic bottles of whisky have been known to sell for prices over £1 million. But how can you be confident that the contents of the bottle are the genuine product? Counterfeit drinks cost the UK economy more than £200 million in lost revenue each year, according to a 2018 study published by the European Union's Intellectual Property Office. New research led by scientists from the School of Physics and Astronomy at St Andrews University, published in *Analytical Methods* (doi.org/d8wg6), has led to the development of a type of spatially offset Raman spectroscopy (SORS) which can see through the bottle to analyse the contents. The challenge in doing so was to record a signal from the contents without recording signals from the glass.

Researchers at St Andrews demonstrated a decade ago that Raman spectroscopy could be used to identify

counterfeit whisky. However, their previous method was hampered by the fact that the alcohol is not the only material to scatter light: the glass of the bottle can create an even bigger signal which dwarfs the signal produced by the contents. Therefore, previous setups required the removal of a small quantity of the liquid for testing. The group of postdoctoral researchers, Holly Fleming, Mingzhou Chen and Graham Bruce, led by Professor Kishan Dholakia, developed a new method to accurately measure the contents of a bottle. Rather than illuminating the bottle with a standard laser beam, the team used a glass element to shape the light to produce a ring of laser light on the bottle surface and a tightly focussed spot within the liquid contents. As the signal from the bottle and the signal from the liquid are at different positions, a detector can be

placed to record only the signal from the liquid, meaning the bottle contents can be assessed without ever opening the bottle.

Professor Kishan Dholakia said: "Personally, I hate it when I have to spare a drop of whisky for validation checks. I'd much rather drink the whole bottle. Laser spectroscopy is a powerful tool for characterising the chemical make-up of many materials, but to use it to characterise alcohol in its original container in this simple way is really exciting."

The approach does not require complex optical setups and, therefore, promises to be easily manufactured for widespread use. If whisky isn't to your taste, the researchers have also demonstrated the method using vodka and gin. Meaning that, in future, you will be able to authenticate your expensive alcohol, without wasting a drop!

NMR techniques for the analysis of paramagnetic materials

Nuclear magnetic resonance (NMR) spectroscopy methods study the structure of diamagnetic molecules very well. In these molecules the electrons are paired together and their NMR spectra

are straightforward to analyse since the signals are usually sharp and in distinctive regions according to the structure of the molecule. However, with NMR methods it is difficult to investigate the

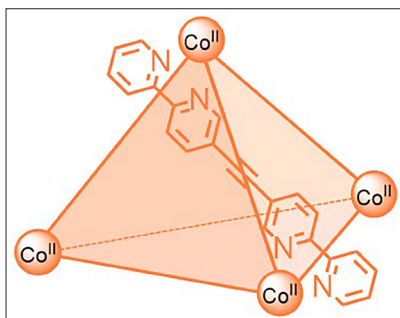
structure of paramagnetic compounds, which have unpaired electrons. These include, for example, some medical contrast agents. They are attracted to external magnetic fields and interfere

with the measurements. Chemists at Kiel University have now succeeded in developing a toolbox of NMR methods which, for the first time, enable detailed structural analysis of paramagnetic complexes in solution. They recently demonstrated the extensive application possibilities of their toolbox in chemistry and beyond in *Angewandte Chemie* (doi.org/d9d9).

"The number of suitable NMR methods for paramagnetic complexes has been limited so far. Structural information is typically lost since the signals are broad and in less predictable regions", explains Anna McConnell, Junior Professor in the Otto Diels Institute of Organic Chemistry at CAU. She is investigating paramagnetic "molecular cages", where several molecules self-assemble into more complex structures with a cavity that can bind other molecules. As a long-term goal, these molecules could be, for example, medicinal substances that are transported and released at particular parts of the body. "But for this we first need more information about the structures of these paramagnetic complexes", McConnell continues.

Together with a research team from the Institutes of Organic and Inorganic Chemistry, McConnell has developed various NMR methods to reliably obtain and interpret NMR data on paramagnetic compounds. Used in combination, the methods of their toolbox provide a comprehensive picture of such molecular structures. In some cases, the results are even better than those with comparable standard methods for conventional diamagnetic compounds, the team found. "Data acquisition for the paramagnetic compounds was much faster and, in some cases, we obtained the structural information in one paramagnetic experiment instead of several experiments for a diamagnetic compound", said McConnell.

The research team carried out detailed investigations on the 500 MHz and 600 MHz spectrometers in the spec-



"Molecular cages" are nano-sized structures that can bind and transport other molecules like medicinal compounds. In order to release them again in a targeted manner, information about their structure and properties is needed, but these paramagnetic compounds are difficult to analyse.

troscopy department of the Otto Diels Institute of Organic Chemistry to determine how to adapt the standard experiments for analysis of the paramagnetic complexes. With this, they produced an instruction manual on how to apply the toolbox to other paramagnetic complexes and spectrometers. "The development of these paramagnetic NMR methods is a big breakthrough for our day-to-day research and we are hopeful that they will help other researchers as much as us", said Marc Lehr, PhD student in McConnell's group and first author of the paper. The research team hopes that this will contribute to the application of these methods in different areas of chemistry and beyond. In their study they demonstrated the toolbox's broad versatility for at least fields from coordination chemistry and spin-crossover complexes to supramolecular chemistry.

As the next step, the research team plans to apply these methods to the analysis of larger and even more complex paramagnetic cages. "Molecular cages whose structures can be changed by irradiation with light are one example of a more complex cage. Using light-responsive cages we might be able to release the guest molecules in a truly targeted manner in the future", McConnell hopes.

Cavity ring-down spectroscopy reveals how corals accumulate pollutants

Marine pollutants are taken up by corals directly from seawater as well as through accumulation in their food

shows research from KAUST using cavity ring-down spectroscopy. This is the first time the approach has been

Are you compliant with the new European Pharmacopoeia 10.0 and USP <857> Standards?

Starna Certified Reference Materials provide an essential tool to achieving data integrity and compliance!



Wide range of available materials to cover all AIQ requirements:

Wavelength accuracy: Deep UV to NIR

Absorbance accuracy & Photometric

Linearity: up to 3.5 A

Stray Light

Instrument Resolution

UKAS Accreditation as a:

Reference Material Producer - ISO 17034

Calibration Laboratory - ISO/IEC 17025

NIST Traceable

Lifetime Guarantee

Fast re-calibration service



Starna

Starna Scientific Ltd

www.starna.com

+44 (0) 20 8501 5550

sales@starna.com



Corals take up marine pollutants directly from seawater as well as through accumulation in their food. © 2020 KAUST-AIMS

used to measure pollutant accumulation.

A hydrocarbon pollutant, phenanthrene, was monitored to see how it accumulates in coral tissue by a team formed by members from Agusti's and Duarte's labs at the Red Sea Research Center, collaborating with researchers at the Australian Institute of Marine Science (AIMS). Coral colonies were grown at the AIMS National Sea Simulator for a fortnight before being exposed to phenanthrene, which is often used as a model for oil pollution. The researchers introduced phenanthrene through two routes. They fed it to microalgae that were then ingested by the corals, and they also

exposed corals to phenanthrene directly in seawater. To track the uptake and accumulation of phenanthrene, they labelled it with ^{13}C and used cavity ring-down spectroscopy to measure the ^{13}C levels in the coral tissues over the course of six days.

The analysis showed that the corals accumulate similar total amounts of phenanthrene, whether via diffusion from the seawater or through uptake in their food. However, the rate of uptake was faster via seawater exposure than from feeding. Ananya Ashok, the lead author of the study, explains that this finding was counterintuitive and points out that uptake is only part of the picture. "It's not

a one-way process. There's a dynamic process of accumulation and elimination constantly happening. It's possible that phenanthrene is being retained more from the diet even though it's taken up at a slower rate", she says.

Understanding the full dynamics of this process is ongoing. The team has experiments planned to investigate pollutant excretion by corals as well as the role of other players, such as copepods, in the food web. "It's important to consider more than one route of accumulation when doing assessments and setting thresholds for these chemicals in natural environments where corals live", says Ashok. "All of the different pathways and dynamics help to develop a more integrated regulatory picture."

This new technique has significant advantages, Agusti explains. "It is an alternative to the use of radioactive isotopes, traditionally used to trace compounds in organisms and food webs." Radioactive isotopes are potentially harmful to the environment. Also, their toxicity makes it challenging to correctly estimate how well marine organisms tolerate pollution. The new technique resolved these risks and makes it possible to run experiments for weeks instead of just hours.

The research is reported in *Ecotoxicology and Environmental Safety* (doi.org/d62d).

Major speed increase for IR spectroscopy

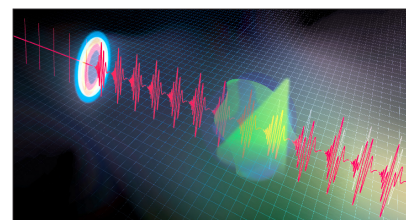
Dual-comb spectroscopy can achieve a measurement rate of 1 million spectra per second. However, in many instances, more rapid observations are required in order to produce fine-grain data. For example, some researchers wish to explore the stages of certain chemical reactions that happen on very short time scales. This drive prompted Associate Professor Takuro Ideguchi from the Institute for Photon Science and Technology at the University of Tokyo and his team to look into and create the fastest infrared spectroscopy system to date.

"We developed the world's fastest infrared spectrometer, which runs at 80 million spectra per second", said Ideguchi. "This method, time-stretch infrared spectroscopy, is about 100 times

faster than dual-comb spectroscopy, which had reached an upper speed limit due to issues of sensitivity."

Time-stretch infrared spectroscopy works by stretching a very short pulse of laser light transmitted from a sample. As the transmitted pulse is stretched, it becomes easier for a detector and accompanying electronic circuitry to analyse it accurately. A key high-speed component that makes it possible is a quantum cascade detector, developed by one of the paper's authors, Tatsuo Dougakiuchi from Hamamatsu Photonics.

"Natural science is based on experimental observations. Therefore, new measurement techniques can open up new scientific fields", said Ideguchi.



Time-stretch infrared spectroscopy. Laser pulses lasting for just femtoseconds are stretched to the nanosecond range. ©2020 Ideguchi *et al.*

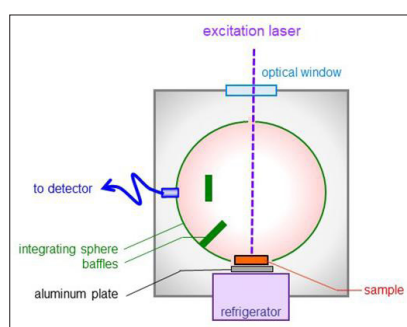
"Researchers in many fields can build on what we've done here and use our work to enhance their own understanding and powers of observation."

They have published the detail of their research in *Communications Physics* (doi.org/d8gh).

Photoluminescence spectroscopy of semiconducting crystals

Tohoku University researchers have improved a method for probing semiconducting crystals using omnidirectional photoluminescence (ODPL) spectroscopy to detect defects and impurities. "Our technique can test materials at very low temperatures and can find even small amounts of defects and impurities", says Tohoku University materials scientist Kazunobu Kojima.

Kojima and his colleagues demonstrated their approach using gallium



The sample is placed outside the integrating sphere and onto an aluminium plate connected to a cooling device. © Tohoku University

nitride crystals. Gallium nitride is a semiconducting crystal that has been used in energy-saving light-emitting diodes (LEDs) since the 2000s. It has interesting optic and electronic properties, making it attractive for many applications, including power-switching devices in electric vehicles. But it can develop defects and impurities during its fabrication, which can affect performance. Currently available methods for testing these crystals are expensive or too invasive. ODPL spectroscopy, on the other hand, is a non-invasive technique that can test the crystals, but only at room temperature. Being able to change the crystal's temperature is important to properly test its properties.

Kojima and his colleagues found a way to set up an ODPL instrument so that the crystal can be cooled. The process involves placing a gallium nitride crystal on an aluminium plate connected to a cooling device. This is placed under an integrating sphere and external light is shone through the sphere onto the crystal, exciting it. The crystal emits light

back into the sphere in order to return to its initial unexcited state. The two lights, from the external source and the crystal, are integrated within the sphere and measured by a detector. The result reveals the crystal's "internal quantum efficiency", which is reduced if it contains defects and impurities, and can be measured even at very low temperatures.

The team's modification—placing the crystal outside the sphere and connecting it to something that cools it—means the temperature change crucially happens only within the crystal and not within the sphere. The scientists were able to measure the internal quantum efficiency of gallium nitride samples using this technique at temperatures ranging from $-261\text{ }^{\circ}\text{C}$ to about $27\text{ }^{\circ}\text{C}$.

"We next plan to use our method for testing other materials, such as perovskites for use in highly efficient solar cells and boron nitride as an atomically thin two-dimensional material", says Kojima.

The details of their new set-up were published in *Applied Physics Express* (doi.org/fcs6).

FT-IR imaging study estimates 10× more plastic in the Atlantic than thought

It had been thought that about 17 million tonnes of plastic had entered the Atlantic Ocean since 1950. However, this new study reported in *Nature Communications* (doi.org/d6xd) indicates that there are about 12 million tonnes just in the top 200 m. Significantly, this figure is only for three of the most common types of plastic litter in a limited size range. This suggests that the supply of plastic to the ocean has been substantially underestimated.

The lead author of the paper, Dr Katsiaryna Pabortsava from the National Oceanography Centre (NOC), Southampton, UK, said "Previously, we couldn't balance the mass of floating plastic we observed with the mass we thought had entered the ocean since 1950. This is because earlier studies hadn't been measuring the concentrations of 'invisible' microplastic particles beneath the ocean surface. Our research is the first to have done this across the entire Atlantic, from the UK to the Falklands.

Co-author, Professor Richard Lampitt, also from the NOC, added "if we assume that the concentration of microplastics we measured at around 200 m deep is representative of that in the water mass to the seafloor below with an average depth of about 3000 m, then the Atlantic Ocean might hold about 200 million tonnes of plastic litter in this limited polymer type and size category. This is much more than is thought to have been supplied. In order to deter-



mine the dangers of plastic contamination to the environment and to humans we need good estimates of the amount and characteristics of this material, how it enters the ocean, how it degrades and then how toxic it is at these concentrations. This paper demonstrates that scientists have had a totally inadequate understanding of even the simplest of these factors, how much is there, and it would seem our estimates of how much is dumped into the ocean has been massively underestimated".

Pabortsava and Lampitt collected their seawater samples during the 26th Atlantic Meridional Transect expedition in September to November 2016. They filtered large volumes of seawater at three selected depths in the top 200 m and detected and identified plastic contaminants using FT-IR imaging. Their study focussed on polyethylene, polypropylene and polystyrene, which are commercially most prominent and also most littered plastic types.

Study on lipid metabolism in human breast tissues by near infrared spectroscopy

Shuo He Yan,^{a,*} Zheng Zhu^a and Joëlle Wallon^b

^aFaculty of Bioscience Engineering, Université Catholique de Louvain, Rue de la Neuville 54/101,1348 Louvain-la-Neuve, Belgium. E-mail: shouheyan12@yahoo.com

^bAnatomie Pathologique, A.N.A.P., Avenue de la Corniche 10, 1310 La Hulpe, Belgium

Introduction

Near infrared (NIR) spectroscopy diagnosis of human breast cancer uses tissue sections similar to those used by pathologists. However, in NIR analysis, both non-stained cancerous and non-cancerous tissue can be assessed. Moreover, NIR diagnosis is dependent upon comparison with normal tissue, which is chosen from a benign fibroglandular non-tumorous zone. Our approach is to try to determine the difference between the two tissue types, and express as frequency (F%) those points in NIR second-derivative spectra that only exist in normal tissue (points of difference).

We have identified four zones within the NIR wavelength region with differences between cancerous and non-cancerous tissue: zones A (1160–1260 nm), B (1740–2070 nm), C (1990–2070 nm) and D (2310–2380 nm): Figure 1(c). Within zone C, there are two points of difference, C1 (2012–2016 nm) and C2 (2044–2048 nm), which are always found in normal (non-cancerous) tissues, so their F% is as high as 100%. Conversely, in cancerous tissue, it is as low as nearly 0%. This difference may originate from either ATP or DNA, since ATP has a C1 at 2016 nm and a C2 at 2048 nm in normal tissues, but DNA has a C1 at 2034 nm and a C2 at 2078 nm in cancerous tissues. Hence why NIR spectroscopy can diagnose tissue types as cancerous or not in human breast tissue qualitatively.¹

The points of difference in zone B include B2 (1764–1768 nm) and B3

(1786–1788 nm), where F% is always as high as 100% in normal (non-cancerous) tissues. However, in cancerous tissues, F% starts at a level of 90–100% in SBR I tissue and then decreases rapidly from 70% to 30% in SBR II sub-type tissue from IIa to IIc, and reaches 0% in SBR III cancerous tissues. The Scarff-Bloom-Richardson (SBR) system grades tumours into three prognostic categories and is used to discriminate the aggressiveness of invasive ductal carcinomas.

This system is applied only to discriminate the aggressiveness of invasive carcinomas. This difference may come from the breast lipids, which are seen in B2 at 1766 nm and B3 at 1788 nm in normal breast tissues. So, breast lipids may enable NIR spectroscopy to diagnose cancerous aggressiveness *quantitatively*.^{1,2}

Our first paper on this topic was published in *Applied Spectroscopy* in 1994³ and the results were also reported at the 6th International Conference on NIR Spectroscopy (ICNIRS). At the 7th ICNIRS in 1995,^{1,2} we reported qualitative and quantitative NIR diagnosis of tissue types and cancerous aggressiveness using F% for a single case or mean frequency MF% for each type.

At the 10th International Breast Disease Congress in 1998,⁴ we introduced chemometric techniques combined with F% to characterise cancerous and normal human breast tissues. The difference in F% between the two tissue types expressed by the t-value in zones B and C is 4.59–4.75 and 7.86–8.02, respectively; the p-values are less than

0.01 and 0.001, respectively, confirming the significance of the results. Moreover, principal component analysis (PCA) can be combined with NIR F% in the calibration, prediction and test sets for qualitative and quantitative analysis. At that meeting, many pathologists were surprised to see that microscopy diagnosis could be replaced by NIR spectroscopy with a 95% precision.

To understand the basis of the NIR diagnosis, we have pioneered ¹⁴C-glucose metabolism research since 1994. In cancerous tissues, glucose escapes the normal metabolic pathway and follows the pentose phosphate pathway, which is why the F% is 0% in zone C. We have also confirmed that the F% is always as high as 90–100% in non-cancerous tissues. Through this process we find that the lipid content decreases as the cancerous aggressiveness increases. The NIR diagnosis of aggressiveness only results from breast lipids, neither ATP nor DNA are involved here. Moreover, we also established the NIR qualitative diagnosis of MCF7/6 breast cancer cells based on cytological evidence.

The purpose of writing this article is to thank Professor John M. Chalmers, who invited me to write a review paper on beer for the *Handbook of Vibrational Spectroscopy*. This invitation gave me the courage to write a book in English on breast cancerous research, which John edited.¹ NIR spectroscopy is a truly captivating field and I was delighted to serve on the organising committees of the 3rd and 4th ICNIRS.

In the process of writing the Chinese version of our English book,¹ which re-analysed the results of past studies, I realised that the results of the glucose metabolism study might lead us to understand the basis for an early diagnosis based solely on body temperature, which would avoid any surgical intervention in diagnosis. This will have to be confirmed by my successors, and I wish them success.

Results and discussions

Differences between cancerous and normal tissues exist in their NIR spectra

Supposing that there are differences in the spectra of cancerous and non-cancerous tissues, it is reasonable to assume that these should be easier to distinguish in spectra recorded from more aggressive cases, such as an invasive ductal carcinoma (IDC), grade SBR III.³

Non-cancerous and normal tissue samples were collected at a distance from the cancerous zone, and cancer-

ous tissue samples were taken from the non-necrotic cancerous zone. The original mean spectra were collected from ten corresponding tissue sections using the NIR $\log_{10}(1/R)$ values, and were recorded from both cancerous (C) and non-cancerous (N) tissues. The spectra of these two types are shown in Figure 1(a). The overlaid second-derivative NIR spectra of N and C tissues from the same SBR III grade case are also shown in Figure 1(b).³

After a comparison of the two overlaid second-derivative spectral profiles from 1100 nm to 2500 nm, we were able to select four zones of bands, A, B, C and D [Figure 1(c)]. To evaluate whether a significant difference existed between the means of the two types of breast tissue, we used the points of difference in nm as the statistical input data from 52 cases (including one MCF7/6 cultured cancerous cell) and 337 tissue sections. After a t-test⁵ for zones C (1950–2122 nm) and B (1730–1822 nm), the highest t-values were 7.86–8.02 and 4.59–4.75, so the p-values are less than 0.001 and 0.01.

Therefore, we proposed that the difference between C1, C2 and B2, B3 points of difference could be used as an NIR spectroscopy diagnostic tool, and we called them diagnostic map C and diagnostic table B, respectively.¹

Evaluation of NIR diagnosis by calibration, prediction and test set

The results of the calibration and prediction series, each from 52 individual cases, are shown in the scores plots in Figure 2(a and b). Hence, we had 28 and 24 mean spectral data values from each series with points of difference of cancerous and non-cancerous cases, respectively.¹

Calibration set

The calibration set consisted of 27 (IDC) SBR grade I, II and III patients (black squares) and one MCF7/6 cancerous cell (black triangle), and 15 SBR grade non-cancerous tissue (open squares) and 9 benign tumour patients with normal tissues (open circles), Figure 2a.

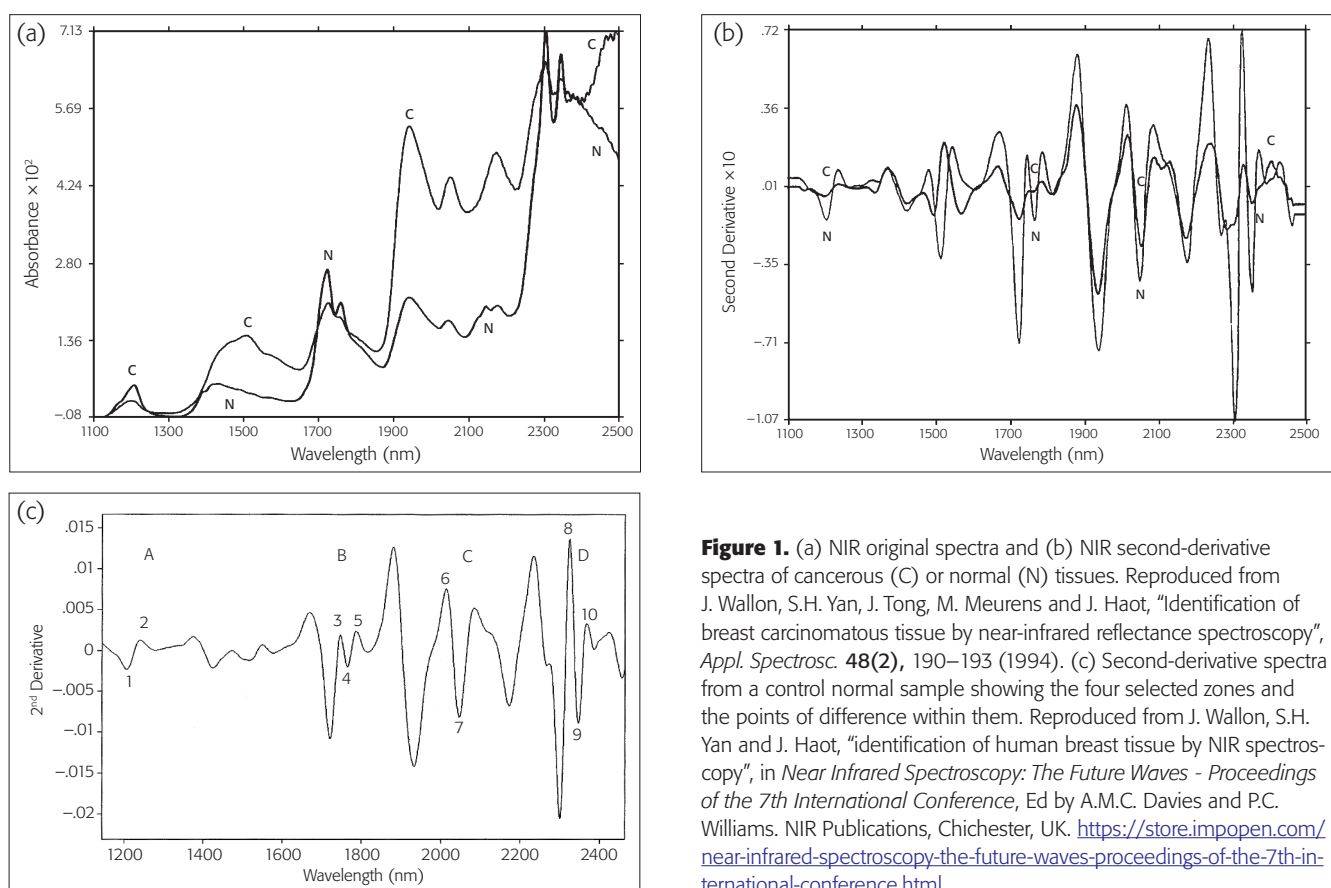


Figure 1. (a) NIR original spectra and (b) NIR second-derivative spectra of cancerous (C) or normal (N) tissues. Reproduced from J. Wallon, S.H. Yan, J. Tong, M. Meurens and J. Haot, "Identification of breast carcinomatous tissue by near-infrared reflectance spectroscopy", *Appl. Spectrosc.* **48(2)**, 190–193 (1994). (c) Second-derivative spectra from a control normal sample showing the four selected zones and the points of difference within them. Reproduced from J. Wallon, S.H. Yan and J. Haot, "Identification of human breast tissue by NIR spectroscopy", in *Near Infrared Spectroscopy: The Future Waves - Proceedings of the 7th International Conference*, Ed by A.M.C. Davies and P.C. Williams. NIR Publications, Chichester, UK. <https://store.impopen.com/near-infrared-spectroscopy-the-future-waves-proceedings-of-the-7th-international-conference.html>

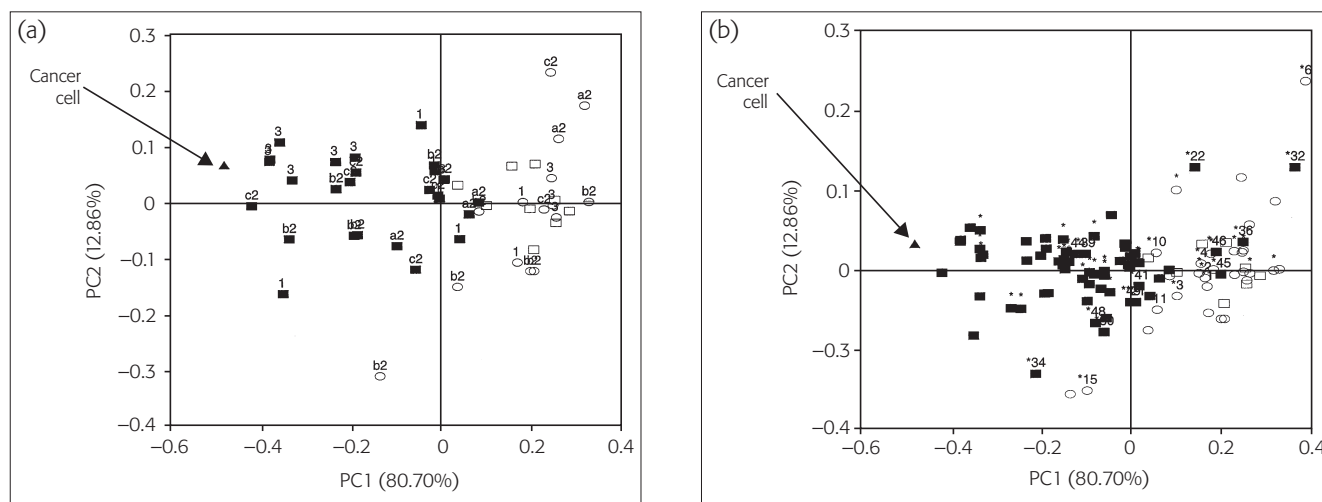


Figure 2(a). The PC1 vs PC2 diagnostic map C for classifying SBR-grade cases. (b) Improvement of Figure 2(a) by using NLM-PCA. © 2009 IM Publications, reproduced from Reference 1 with permission.

Figure 2(a) shows the best PCA map C, obtained using pre-processing with range-scaling, in which the first two PCs together accounted for 93.56% of the original variances: PC1 for 80.70% and PC2 for 12.86%.

In Figure 2(a), all 27 (IDC) cases are closest to the MCF7/6 cancerous cell, followed by the aggressive cases from SBR III (3), IIc (c2), IIb (b2) and SBR I (1) patients. All normal control and non-cancerous cases lie furthest away from the MCF7/6 cancerous cell position. The incorrectly or borderline classified cases correspond to 2% (1/52) and 6% (3/52) for non-cancerous and cancerous cases, respectively. However, if the same input data were treated by non-linear regression first and then plotted with PCA, the mapping error decreased from 0.012060 to 0.006142. Then it would be easy to determine whether both cases were just borderline or not.¹

Prediction set

Figure 2(b) shows results for the prediction set. It has been overlaid on Figure 2(a) to validate the calibration. We have developed a software package—CAIBT (Chemometric Approaches to Identify Human Breast Tissues, not published)—to automate the testing of individual cases. The NIR spectral data are input and the case type is determined by its position compared to the calibration samples;⁶ the closer, the higher is

the resemblance. In conclusion, the NLM-PCA map can diagnose higher or lower-grade aggressive SBR cases with an acceptable error rate.^{1,7}

Test set

The test set was used to validate the NIR procedure:¹ for example, the ability of the procedure to distinguish malignant from benign breast cases, and the most malignant aggressive cases from the lesser ones. Input data included 35 cases of fibroadenoma and control, non-malignant, surrounding tissues. In total,

92 cases are shown in Figure 3, which shows map C for the best PCA diagnosis.¹ All input data was pre-processed by range scaling, combined with mean centring. Furthermore, 96.22% of the original variances are accounted for, PC1 for 84.37% and PC2 for 11.85%.

The 33 malignant tumour score points (*) from aggressive higher-cystosarcoma phyllodes (hCP) malignant tumour cases are clearly located on the right of the map along with the MCF7/6 cancerous cell score (+) point. The five less-aggressive lower-cystosarcoma phyllodes (ICP)

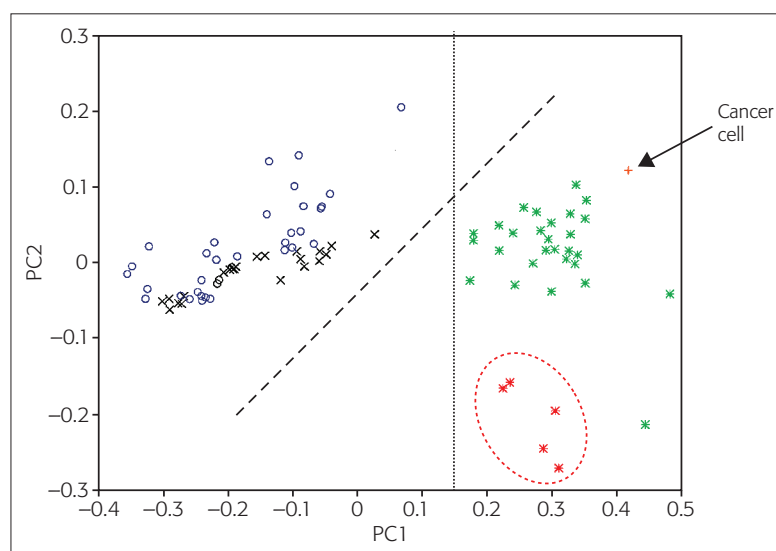


Figure 3. The PC1 vs PC2 diagnostic map C to classify breast tumour types. FG: fibroglandular (normal); FA: fibroadenoma (benign); MA: non-malignant; Control MA: control non-malignant surrounding tissues; Cancer: MCF7/6 cancer cell. © 2009 IM Publications, reproduced from Reference 1 with permission.

malignant tumour cases (*) are located towards the bottom of the right half; a dashed ellipse has been drawn around these. The score points from control normal or non-malignant (o) and benign (x) tissues are positioned separately, mostly in the left part of map C. Normal and non-cancerous (o) samples have a tendency to lie closer to the top of map C, while benign tumour score (x) points are more often located nearer to the middle of Figure 3. The boundary line through PC1 = 0.15 (from the bottom to the top) clearly separates the MCF7/6 cancerous cells and all malignant tumour score points in the right part of Figure 3, with all other types of tissue being situated in the left part.

NIR diagnostic tools in zone C and B are based on ATP or breast lipids

NIR diagnostic tools in zone C are based on ATP, in which normal tissues have C1 at 2016 nm and C2 at 2048 nm. ATP spectra were recorded using the following procedure: about 10 mg ATP chemical reagent (Roche Biochemical, Inc., purity 100%) was sandwiched between two glass coverslips, then placed between two 50-mm diameter glass-fibre filters (Millipore AP 4007), each having a 20 mm diameter hole in the centre and mounted between two 55-mm diameter glass windows. The assembly was then placed in the reflectance sample cup. The spectra of ATP were measured from 1100 nm to 2500 nm at wavelength intervals of 2 nm. A background reference spectrum was obtained by recording the NIR spectrum under the same conditions as the sampling assembly, but without ATP being present. The ATP original spectrum was transformed into the second derivative NIR spectrum by NSAS soft-

ware (Foss). The NIR spectra of DNA (also RNA) were recorded in the same procedure as for ATP.^{1,8}

The spectra of MCF7/6 cells were recorded by the following procedure: MCF7/6 cells were first washed with physiological water and then centrifuged for 10 min at 5000 rpm and 10 °C. Then washed again using distilled water and centrifuged again under the same conditions. A suspension drop containing about 1–2 mg of fresh cells, after drying at room temperature to form a thin uniform film, was placed between a pair of cover slips, then sandwiched together and placed in the reflectance sample cup. NIR reflectance spectra of MCF7/6 cells were recorded for ATP and DNA.^{1,8}

NIR diagnostic tools in zone B are based on breast lipids, with B2 found at 1766 nm and B3 at 1788 nm in normal tissues. That is why zone B can diagnose cancer aggressiveness quantitatively by using F% or MF%.^{2,9} The breast lipid spectra were recorded as follows. A cancerous tissue section with SBR I grade was maintained at about 95 °C to 100 °C for five minutes, after which a drop of breast lipids was revealed in the form of an oil drop that was yellow in colour. This was then collected using a glass Pasteur pipette (230 mm, VWR International SAS) and placed between a pair of cover slips for NIR analysis. The NIR second-derivative spectra of these breast lipids are within the range of the B2 and B3 significant points of difference of normal human breast tissues, as collected from the non-tumour zone of benign fibroglandular tumours (see Table 1).

Table 1 is a summary of the elementary reasons why NIR spectroscopy delivers diagnostic evidence as well as the motivation for all our research.⁵ In the corresponding NIR spectra, there are

two peak positions for DNA in zone C at 2034 nm and 2078 nm, but for MCF7/6 breast cancer cells it is at 2024 nm and 2058 nm. Both are shifted and far away from ATP or non-cancerous tissues. Therefore, we can identify cancerous cases from non-cancerous cases using the NIR diagnostic tool of C1 and C2.

ATP can also be a valuable tool for the diagnosis of breast cancer: in cancerous tissue, ATP is absent, but DNA exists, so the F% in zone C is always 0%. However, the F% in zone B is as high as 90–100% in SBR I cancerous tissue, decreases rapidly from 70% to 30% in SBR II and to 10–0% in SBR III cancerous tissue.¹ This means that breast lipids are a valuable tool for the diagnosis of breast cancer aggressiveness.¹

The NIR spectra of fresh MCF7/6 cells are similar to cancerous tissues, but are completely different from those of normal or non-cancerous tissues.⁵

Evaluation of NIR tools based on ¹⁴CO₂ production ratios Vn and Vc^{5,6}

In 1998, we discovered that glucose metabolism changes when human breast cancer develops. In order to elucidate the complex metabolic pathways of glucose, it is often necessary to use selective-positioning of the radioisotopic label. For example, 1-¹⁴C-glucose (in which the first carbon is labelled), 6-¹⁴C-glucose (in which the sixth carbon is labelled) or U-¹⁴C-glucose (which is uniformly labelled; all carbons from positions one to six are labelled).

If ¹⁴C-glucose follows a different metabolic pathway in cancerous and non-cancerous tissues, this will be reflected in the ¹⁴CO₂ production ratios, Vc or Vn, respectively. If (Vn-1/Vn-6) = 1, it will have followed the Embden–Meyerhof

Table 1. Comparing the NIR diagnostic tool with test-points of breast lipids, ATP or DNA.

Test points	Normal tissue (nm)	Non-cancer tissue (nm)	Breast lipids (nm)	ATP (nm)	Cancerous tissue (nm)	MCF7/6 cancer cells (nm)	DNA (nm)
C1	2012–2016	2012–2016	—	2016	2018–2022	2024	2034
C2	2044–2048	2044–2048	—	2048	2052–2058	2058	2078
B2	1764–1768	1764–1768	1766	1774	1750–1762	1730	1752
B3	1786–1788	1786–1788	1788	1798	1770–1784	1782	1776

process and the Krebs cycle pathway, and tissue is normal or non-cancerous. If $(Vc-1/Vc-6) > 1$, it will have followed the pentose phosphate pathway and is cancerous tissue.

Of the seven patients (aged from 41 to 60), one had a fibro-glandular benign tumour and two each had SBR I, SBR II and SBR III grade tumours. We wanted to determine the relationship between F% and the $^{14}\text{CO}_2$ production ratios (Vc or Vn).¹⁰

Table 2 shows the F% analyses of 10–15 tissue sections of both cancerous and non-cancerous tissue. The MF% data (in brackets in Table 2) are given for reference. These were collected from six benign tumours and IDC SBR I, II and III cases. In total, 27 cases of normal or non-cancerous tissues. The MF% data were collected from 35 different types of tumour cases, and from SBR I, II and III IDC cases; in total 34 cases¹⁰ of cancerous tissues are listed in Table 2.

The $^{14}\text{CO}_2$ production ratios (Vc or Vn) for the same seven patients^{5,6} were collected with the following procedure. For each type of tissue, about 200 mg (± 10 mg) was used, which was obtained from breast resections and then immersed in physiological water at about 10 °C. The specimen was first removed from the fat and dried with Whatman 2 filter paper. The enzymatic activity of the tissue remained constant over about 36–40 h. The tissue sample was then washed with physiological

water and distilled water before analysis. Various labelled forms of ^{14}C -glucose (2 μCi) from Service des Molécules Marquées, France, were added separately to each sample for a final glucose concentration of 0.5 μmol . The resulting suspensions were incubated at 37 °C for 2 h under atmospheric conditions. The $^{14}\text{CO}_2$ production was measured as $V = \text{nanomole min}^{-1} \text{g}^{-1}$ of fresh tissue.

Comparing the results from Table 2, the Vn-1/Vn-6 data ratios range from 0.97 (1.421/1.462) to 1.01 (0.513/0.505) and 1.20 (0.107/0.089) for SBR I, II and III non-cancerous tissue, but 1.48–1.49, 2.33–2.90 and 6.09–9.74 for SBR I, II and III cancerous tissues. These results clearly confirm that F% is 0% due to DNA replacing ATP in zone C. However, F% is 90–100% in SBR I, decreasing from 70% to 30% for SBR IIa to IIc and reaching 0% for SBR III cancerous tissue in zone B. These results clearly confirm that the F% of zone B decreases as cancer aggressiveness increases, and that this is due to changes in breast lipids. Moreover, the F% data of SBR I cancerous tissues are 0% in zone C, and the $1\text{-}^{14}\text{CO}_2/6\text{-}^{14}\text{CO}_2$ ratios of the same tissues are higher at 1.5, so the two methods confirm that SBR I is cancerous. However, in zone B, the F% of SBR I cancerous tissues is still over 90%, for SBR II it becomes 70–30% and for SBR III 0%. This shows that lipid metabolism changes after changes in glucose metabolism changes.

^{14}C -glucose Vn data may allow early diagnosis by NIR⁷

Using standardisation of ^{14}C -glucose Vn data, it looks possible to develop a method based on NIR spectroscopy to diagnose breast cancer in its early stages. Standardisation is a common statistical tool and widely exploited in difference series data values. In our case, first, we define the normal breast tissue Vn data as 100 and establish it as a comparable standard. Then all non-cancerous tissue input data are standardised. For example, using the three types of ^{14}C -glucose,⁸ normal tissue input Vn data are 0.882, 0.538 and 0.560 in Table 3, after standardisation they all become 100. However, for the same three types of ^{14}C -glucose for SBR I non-cancerous tissue, the input data are 1.323, 0.919 and 0.911. After standardisation they become $(1.323/0.882) \times 100 = 150$, $(0.919/0.538) \times 100 = 171$ or $(0.911/0.560) \times 100 = 163$ and so on, as shown in Table 3.

The $^{14}\text{CO}_2$ production Vn data are shown in the left-hand of the pairs of columns for each of the three types of ^{14}C -glucose in Table 3 and on the right after standardisation: 150 and 244, 171 and 264, 163 and 261 from the $\text{U-}^{14}\text{CO}_2$ and $1\text{-}^{14}\text{CO}_2$ and $6\text{-}^{14}\text{CO}_2$, respectively, for two cases of SBR I non-cancerous tissues. However, the corresponding non-cancerous tissue data for SBR II are 95 and 89 for $\text{U-}^{14}\text{CO}_2$, and only 95 or 90 for $1\text{-}^{14}\text{CO}_2$ or $6\text{-}^{14}\text{CO}_2$ non-cancer-

Table 2. Relationship between F% (MF%)² and $^{14}\text{CO}_2$ ratios of Vn or Vc in SBR tissues.

Pathological cases types: N or C	F% or (MF%) in zone B or C				^{14}C -glucose ratio between Vc and Vn for:		
	C (cancerous)		N (normal)		U- $^{14}\text{Cglu}$.	1- $^{14}\text{Cglu}$.	6- $^{14}\text{Cglu}$.
	C	B	C	B	Vn-U, Vc-U	Vn-1, Vc-1	Vn-6, Vc-6
Normal tissue:	F% (MF%)				Vn=0.901 and 0.862, mean 0.882		
	0 (85)	80 (85)	100 (100)	100 (100)	Vn-U & Vc-U	Vn-1 & Vc-1	Vn-6 & Vc-6
Vn or Vc from:							
SBR I-a	0 (0)	80 (86)	90 (100)	90 (100)	1.323 & 2.800	0.919 & 1.992	0.911 & 1.341
SBR I-c	0 (4)	70 (81)	90 (88)	90 (97)	2.155 & 3.135	1.421 & 2.817	1.462 & 1.899
SBR II	0 (2)	70 (60)	80 (84)	90 (94)	0.836 & 2.389	0.513 & 3.092	0.505 & 1.330
SBR II-c	0 (0)	30 (20)	80 (78)	90 (72)	0.784 & 2.547	– & 4.092	– & 1.412
SBR III	0 (0)	10 (8)	70 (66)	80 (78)	0.402 & 1.840	0.107 & 4.825	0.089 & 0.793
SBR III	0 (0)	0 (0)	60 (56)	70 (68)	0.218 & 2.263	– & 7.042	– & 0.723

Table 3. Standardised ^{14}C production Vn data in non-cancerous tissues.

Tissue type	U- ^{14}C -glucose		1- ^{14}C -glucose		6- ^{14}C -glucose	
Normal tissue (Vn)	0.882	as (100)	0.538	as (100)	0.560	as (100)
SBR I (Non-cancerous)	1.323; 2.155	(150; 244)	0.919; 1.421	(171; 264)	0.911; 1.462	(163; 261)
SBR II (Non-cancerous)	0.836; 0.784	(95; 89)	0.513	(95)	0.505	(90)
SBR III (Non-cancerous)	0.402; 0.218	(46; 25)	0.107	(20)	0.089	(16)

as: after standardisation

ous tissues. The ^{14}C ratios decreased rapidly in SBR III cases, only 46 and 25 from U- ^{14}C , and 20 and 16 from 1- ^{14}C or 6- ^{14}C . So, the Vn data for SBR I (244–264) are about 3–16 times higher than same normal tissue (100) or non-cancerous tissue of SBR II (89–95) or SBR III (46–16). This result reports an important piece of information, which suggests that ^{14}C -glucose catabolism in non-cancerous SBR I cases will be quantitatively higher than normal and lower than non-cancerous SBR II or SBR III. Breast cancer development times from SBR I to SBR II are a minimum of three months, ignoring any influence from chronic diseases. If after this period the body temperature suddenly drops, this may suggest that SBR I has progressed to SBR II or SBR III, which may help in the development of a method to use NIR spectroscopy to provide early diagnosis by monitoring body temperature.

Why did we not recognise this important information before? First, we only used normal tissue as a standard to establish a diagnostic tool. Second, we accepted the point of view of our pathologist, who never paid attention to normal tissue.⁷ Thanks to standardisation, we have made this discovery and will hopefully be able to develop NIR-based, early diagnosis tools.

Conclusions

This article introduces NIR spectroscopy as an efficient method to compare ^{14}C -glucose metabolism and pathological diagnosis. However, as we have presented elsewhere,⁸ only NIR spectroscopy can evaluate the metabolism of lipids and glucose from a quantitative and qualitative point of view. Moreover, NIR spectroscopy is accurate, fast, cheap

and easy to commercialise. We believe that they all have an excellent future. We believe that skin cancer and pigmented cancer could easily benefit from this method, because it is easy to find normal tissue for modelling, and there is no need research samples to be obtained through surgery. In this way, we could develop an early temperature test to discover SBR I breast cancer.

References

1. S.H. Yan and J. Wallon, *Identification of Human Breast Cancer by NIR Spectroscopy and Radiorespirometry*, Ed by John M. Chalmers. IM Publications, Chichester, UK (2009).
2. J. Wallon, S.H. Yan and J. Haot, "Identification of human breast tissue by NIR spectroscopy", in *Near Infrared Spectroscopy: The Future Waves*, Ed by A.M.C. Davies and Phil Williams. NIR Publications, UK, pp. 337–342 (1996). https://www.impopen.com/book-summary/978-1-906715-20-5_ch59
3. J. Wallon, S.H. Yan, J. Tong, M. Meurens and J. Haot, "Identification of breast carcinomatous tissue by near-infrared reflectance spectroscopy", *Appl. Spectrosc.* **48(2)**, 190–193 (1994). <https://doi.org/10.1366/0003702944028542>
4. J. Wallon, S.H. Yan, J. Mayaudon and J. Haot, "Characterization of carcinomatous and normal human breast tissues by near infrared spectroscopy (NIRS) combined with chemometric techniques", *Proceedings of the 10th Int. Cong. on Senology Breast Diseases, Oporto, Portugal, May 31 to June 4, 1998*, Ed by J. Cardoso da Silva. Monduzzi Editore Pub., Italy, pp. 691–694 (1998).
5. J. Mayaudon, S.H. Yan and J. Wallon, "A proposed estimate of the tumor aggressiveness of human breast cancer using radiorespirometry," *IUBMB Life* **45(6)**, 1073–1079 (1998). <https://doi.org/10.1080/15216549800203292>
6. S.H. Yan, J. Wallon and J. Mayaudon, "Rate of ^{14}C production from variously labeled forms of ^{14}C -glucose in human breast invasive ductal carcinoma tissues", *IUBMB Life* **48(4)**, 409–411 (1999). <https://doi.org/10.1080/713803528>
7. S.H. Yan, J. Mayaudon and J. Wallon, "Identification of the Lower Cancerous Aggressiveness as SBR in Human Breast Tissues by using Radiorespirometry", *The Breast Journal* **4(Supplement 1)**, 403–S64 (1998).
8. J. Wallon, S.H. Yan, M. Meurens and J. Haot, "Spectroscopie proche infrarouge de tissus mammaires normaux et carcinomateux et corrélation avec l'anatomie pathologique", in *4^{ème} Journée Francophone de Cytologie Clinique*, Bruxelles, Belgium [in French] (1992).
9. S.H. Yan, J. Mayaudon and J. Wallon, "NIR prediction and biochemical properties in human breast invasive carcinoma tissues", *J. Near Infrared Spectrosc.* **6(A)**, 273–277 (1998). <https://doi.org/10.1255/jnirs.207>
10. S.H. Yan and J. Wallon, "Estimate of human breast invasive ductal carcinoma aggressiveness by ^{14}C production from variously labeled forms of ^{14}C -glucose", *Proceedings of the 6th National and International Breast Cancer Congress*, September 7–9, 2000, Tianjin, China, pp. 8 (2000).

Column properties that make an impact on ion chromatography

Carl Fisher and John Guajardo

Thermo Fisher Scientific, Sunnyvale, CA, USA

For the separation of ionic species, ion chromatography (IC), a type of liquid chromatography, is the method of choice. The most critical component of this technique is the separation column, which is selected based on factors that include the specific analytes of interest, the sample type and the required detection levels. This article outlines the column parameters that impact the separation of charged species in solution using ion-exchange chromatography and the developments that have continued to redefine what is possible with an IC system.

Role of columns in ion chromatography

The characteristics of a separation column are one of the most critical considerations for obtaining optimal results from an ion chromatography (IC) system (Figure 1). The column dictates how well the ionic components of a solution are separated, which is essential for confident peak integration. It determines whether analytes will be only crudely detected or quantified in the parts per billion (ppb) range.

The quality of the separation is influenced by multiple factors, some of which can be varied by adjusting the method parameters and others that are fixed by the properties of the column. Chromatographic conditions that the system operator has direct control over include eluent concentration, flow rate, temperature and sample loading volume/concentration. Because IC is limited to just a few eluents, choosing a column with the right selectivity is critical for achieving a desired separation, especially when analytes are of the same charge. The initial column selection is the focus of this article, and the characteristics that will be discussed are particle size, surface area, resin surface chemistry and format. The interplay of the instrument method variables along with the selected column's stationary phase dictates how well the analytes

are separated, ultimately determining the quality of the chromatographic data obtained and the quantification that can be attained.

Early IC column development

The earliest IC separations used a lightly sulfonated (R-SO₃⁻) styrene-divinylbenzene (DVB) polymer (stationary phase) to create a cation-exchange surface and dilute hydrochloric acid as the eluent (mobile phase).¹

Styrene-based polymers were preferred over the silica-based materials that were commonly used in High Performance Liquid Chromatography (HPLC) due to their superior chemical stability. The first widely used anion-exchange stationary phases were created by coating a surface-sulfonated styrene-

DVB resin with a suspension of colloidal ion-exchange resin bound to the cation-exchange surface.

These columns originally used phenate-based eluents, but a hydroxide-based mobile phase was a more attractive option because of the low background achievable and the potential for use in gradient elution. However, the low eluting strength of hydroxide eluents meant high concentrations were needed to displace all the anionic analytes that were bound to the resin. This required frequent offline regeneration of the packed bed suppressors that were in use at the time, causing a bottleneck for throughput. Another concern with the use of manually prepared hydroxide-based eluents was the inability to eliminate carbonate impurity, which, by itself, has a strong analyte displac-

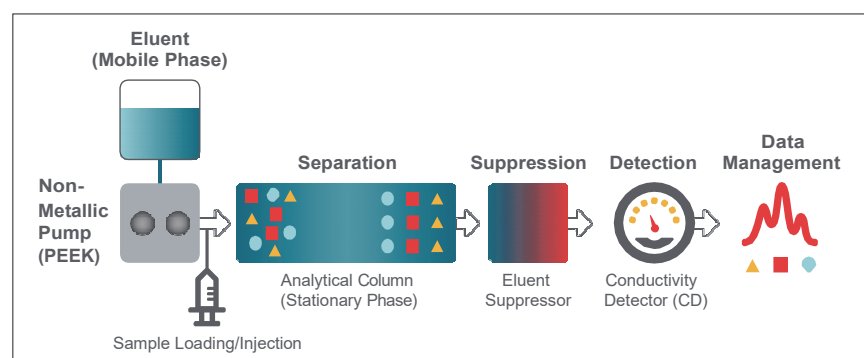


Figure 1. Schematic diagram of an IC system. Polyetheretherketone, PEEK.

ing potential, creating an unpredictable elution profile. When carbonate-based eluents were tried their strong elution potential meant that lower concentrations could be used, and, thus, fewer suppressor regenerations were required. This relative ease of use resulted in their widespread adoption and production of columns with peak separations optimised for use with carbonate eluents. As suppressor technology matured to the point where offline regeneration was no longer required and adequate suppression capacity was available, hydroxide-based eluents became a much more favourable mobile phase because of their ability to be suppressed to water. This is the ideal background for conductivity measurements, producing the best signal/noise ratio to achieve the lowest limits of detection with conductivity detection (CD). With the development of electrolytic eluent generation (Reagent-Free IC, RFIC), on-demand production of hydroxide-based eluent from deionised water meant that carbonate contamination was no longer an issue. An added benefit is that highly reproducible gradients, which focus peaks to yield greater chromatographic peak capacity, can be produced without the need for a proportioning pump.

Achieving greater efficiency: resin particle size

The first resins used for IC were approximately 35 μm in diameter. Modern IC stationary phase particles from Thermo Scientific range in size from approximately 9 μm to 4 μm . The development of smaller particles in both HPLC and IC columns was driven by the increased column efficiency that is obtained, and extension of the range of flow rates at which this is maintained, giving users more flexibility in optimising their method. What this means to the chromatography is taller and narrower peaks that are better separated, resolving closely eluting analytes that could previously not be distinguished and facilitating peak integration, which leads to more accurate quantification.^{2,3}

A consequence of developing ever smaller sized particles is the need to

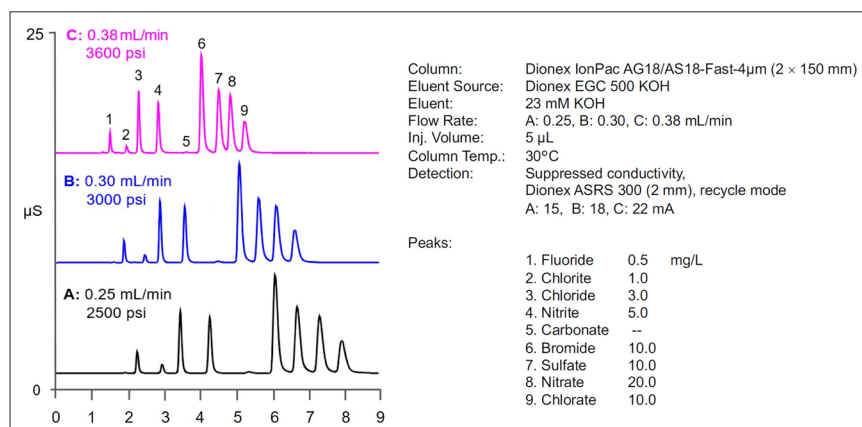


Figure 2. Reduction in run time achieved using higher flow rates in combination with a reduced length, 4 μm resin particle column.

develop, in parallel, instrumentation that can handle the higher backpressures that arise. Thermo Scientific™ Dionex™ High Pressure IC (HPIC) systems meet this challenge with pumps, valves and consumables that can tolerate backpressures of up to 5000 psi, which allow users to take full advantage of a column's potential. While some vendors reduce the column length to achieve shorter run times, Thermo Scientific combines a shorter column with smaller particle resins to not only achieve faster run times, but also maintain chromatographic efficiency and resolution (Figure 2).

Increasing column capacity: resin porosity

The initial polystyrene-DVB particles used for IC were non-porous and resulted in columns with relatively low capacity. To handle high analyte concentrations, improve the resolution of weakly retained ions, analyse high-ionic strength samples, and to load a higher sample volume without overloading and peak broadening, high column capacity is needed. To achieve this, resins have been engineered with varying amounts of porosity, allowing more surface area per particle to be exposed to the mobile phase and, thereby, providing more opportunities for sample analytes to bind to the surface, increasing capacity. This is exemplified by the change in core resin used for Thermo Scientific™ Dionex™ IonPac™ AS11-HC particles from microporous as in Thermo Scientific™ Dionex™ IonPac™

AS11 (<10 Å pores, Figure 3A) to supermacroporous (2000 Å pores, Figure 3B). The larger pores present more surface for the agglomeration (attachment) of latex particles (80 nm Thermo Scientific™ Dionex™ MicroBead™ resin), increasing the column capacity from 45 μeq to 290 μeq (>500%) for a 4 × 250 mm column.

Altering selectivity: resin surface modification

The surface of organic polymers used in anion-exchange resins can be functionalised (i.e., have their properties altered) using a two-step process of 1) addition of a chloromethyl group to the aromatic resin skeleton, followed by 2) amination with a tertiary amine. For cation-exchange resins, functionalisation consists primarily of surface sulfonation via reaction with concentrated sulfuric acid or carboxylation via reaction with carboxylic acid (see Reference 4 for a comprehensive review).

While the first stationary phases consisted of lightly sulfonated (R-SO₃⁻) polystyrene-divinylbenzene (PS/DVB) polymer, the surface properties of IC resins used today are modified by employing multiple strategies that include encapsulation, polymeric grafting, chemical derivatisation, step-growth and agglomeration (Figure 4). The precise way in which the stationary phase is synthesised and functionalised enables the selectivity of each resin to be finely tuned to meet specific application requirements.

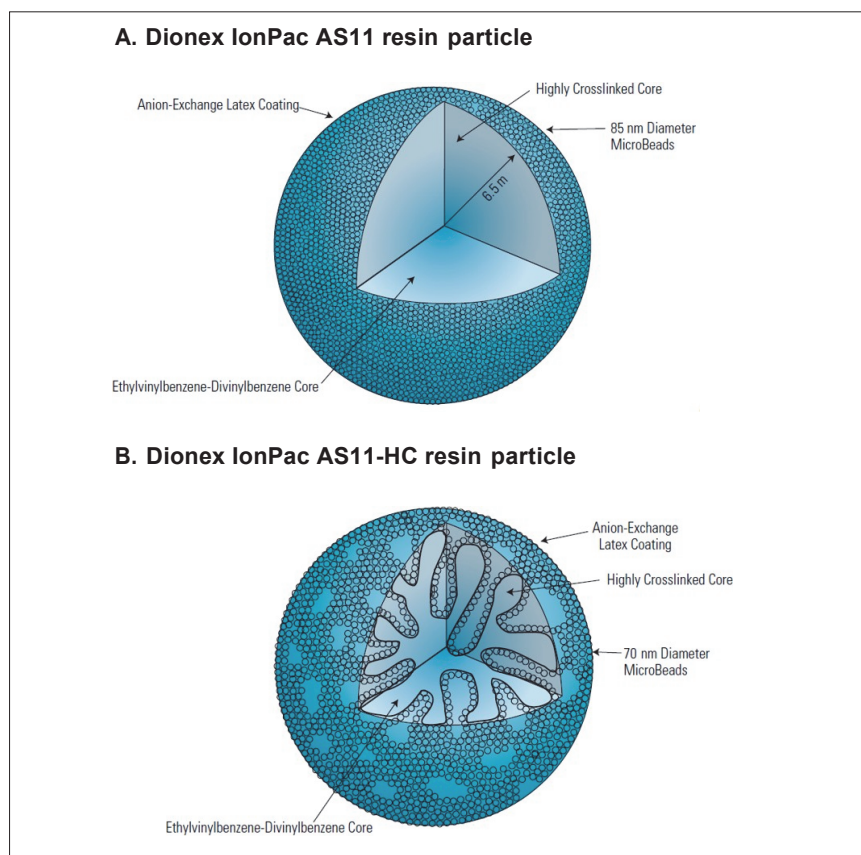


Figure 3. Comparison of Dionex IonPac AS11 and AS11-HC resin particle structures.

Column formats

Separation columns are available in multiple formats that vary by inner diameter (i.d.) and length. The column diameter used is primarily determined by the chromatographic system's properties, the sensitivity required and the sample volume (Table 1). Most standard IC systems can run analytical (4 mm i.d.) and microbore (2 mm i.d.) columns. However, Thermo Scientific™ Dionex™ ICS-4000 and Thermo Scientific™ Dionex™ ICS-6000 HPIC systems are the only IC systems currently available that are capable of running capillary (0.4 mm i.d.) columns. The pumps used in both systems reliably and precisely deliver flow rates in the μLmin^{-1} range. They are equipped with components such as suppressors, eluent generators, degas assemblies and carbonate removal devices that are specifically designed for capillary flow rates and volumes. The low sample volumes and eluent consumption of capillary IC result in minimal waste disposal requirements and allow the system to be run continuously. Consequently, these systems are always

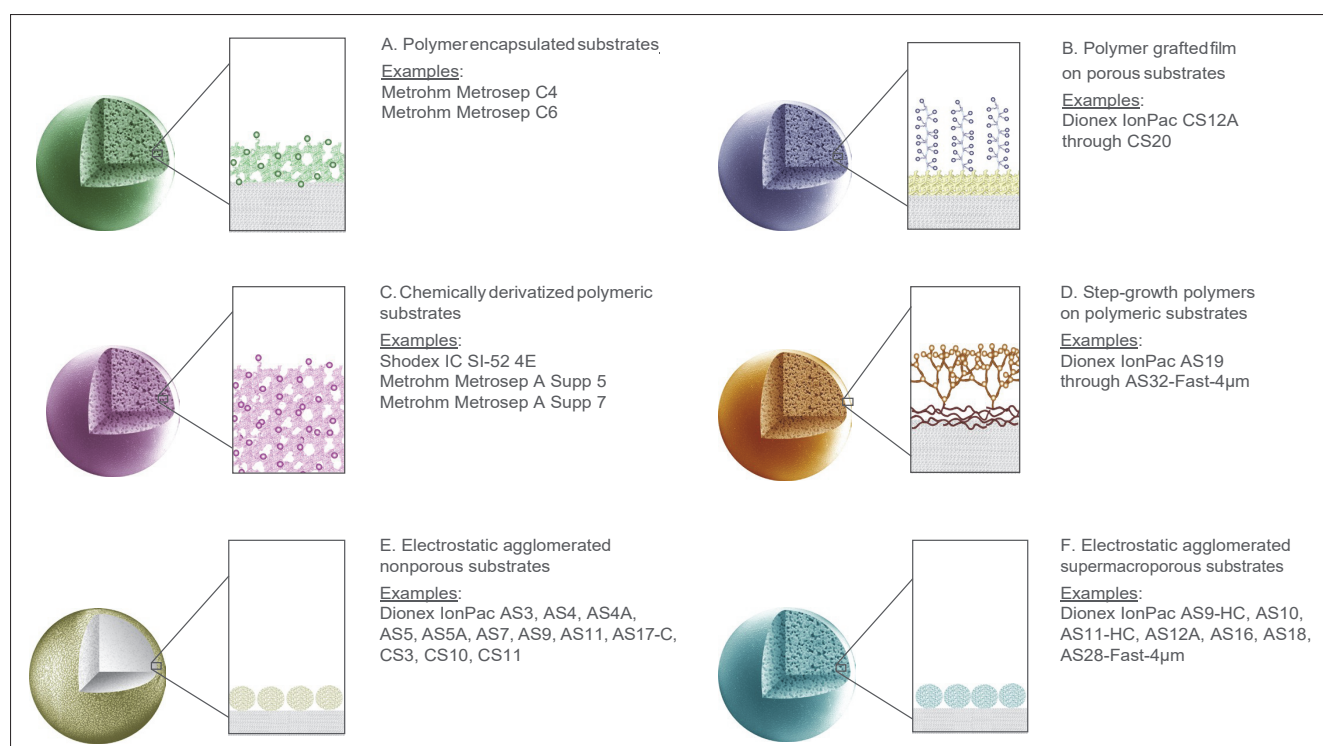


Figure 4. Commonly used IC column stationary-phase architectures.

SPONSORED ARTICLE

Table 1. Comparison of parameters for IC column formats.

	Analytical	Microbore	Capillary
Column i.d. (mm)	4	2	0.4
Flow rate (mLmin ⁻¹)	1.0	0.25	0.01
Injection volume (μL)	10	2.5	0.1
Eluent consumption/waste generated (L/month)	43.2	10.8	0.432
Best suited for	<ul style="list-style-type: none"> Established procedures with specific requirements that cannot be readily changed 	<ul style="list-style-type: none"> Standard applications Reduced eluent consumption and waste generation Low-level determinations 	<ul style="list-style-type: none"> Minimal sample/eluent consumption; and waste generation "Always-ready," minimised turnaround time Routine applications

Table 2. Comparison of IC column resin types from various vendors.

		Vendor A	Vendor B	Thermo Scientific
Particle size	≤4 μm	—	1	10
	5–12 μm	14	11	40
Capillary columns (0.4 mm i.d.)		—	—	31
Anion columns (eluent type)	Carbonate	8	6	11
	Hydroxide	—	—	24
	Other	—	2	—
Cation columns		6	4	15
Total columns		14	12	50

ready to run samples because there is no need for extensive equilibration prior to the start of a run, which is required with standard bore systems that are regularly put into standby mode to save eluent and reduce waste. There are more than 30 Thermo Scientific capillary anion- and cation-exchange columns, many in 4 μm particle size (Table 2).

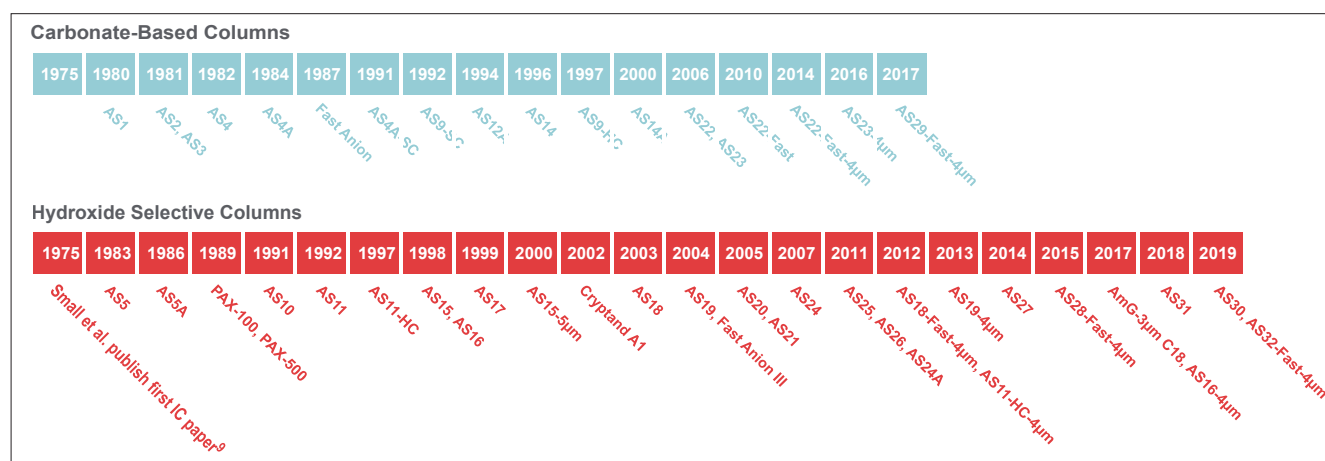
A history of innovation

From the very first "Anion Separator Column" to the present day Thermo Scientific™ Dionex™ IonPac™ AS32-Fast-4 μm column, Thermo Fisher Scientific has been dedicated to continually developing new columns to meet the ever-changing needs of our customers, who are tackling new analytical

challenges every day (Figures 5 and 6, Reference 5).

One example of column development driven by customer needs is the recently released Thermo Scientific™ Dionex™ IonPac™ AS31. One of the limitations with the analysis of haloacetic acids (HAAs) in drinking water using US EPA method 557⁶ is the analysis time of approximately one hour per sample. This limits the number of samples that can be analysed in a day, increasing the cost per sample. Customers expressed a desire for a more economical method.

To address this need, the column chemistry was modified to change the elution order of sample constituents so that the components that were directed to waste or to the mass spectrometer for detection could be grouped more efficiently. The net result was a 39% decrease in the overall run time leading to a significant reduction in cost per sample and time to result.⁷

**Figure 5.** Thermo Scientific Dionex anion-exchange IC column development timeline.

SPONSORED ARTICLE

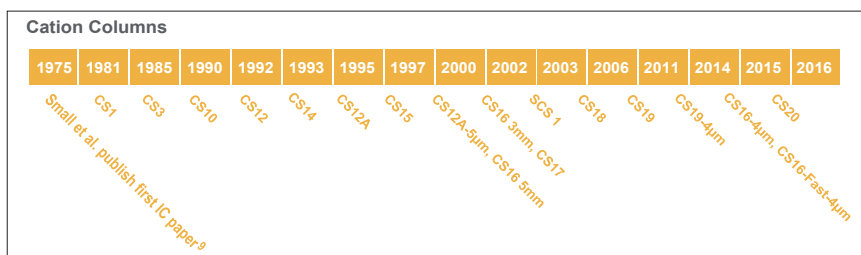


Figure 6. Thermo Scientific Dionex cation-exchange IC column development timeline.

Another example of solid-phase modifications that resulted in greater ease of use is the optimisation of the surface properties of the Thermo Scientific™ Dionex™ IonPac™ CS17 column resin so that it does not require the use of an organic eluent modifier to resolve amines and alkanolamines.⁸ Aside from making manual eluent preparation more straightforward, a RFIC system can now be used, which further simplifies the operation, obtaining precise, reproducible results.

The history of innovation by Thermo Fisher Scientific is exemplified not only by the regularity of new column introductions each year, but also by the number of patents that they have been issued for developments in IC column technology, which is unmatched in the industry (Figure 7).

Summary

The continual response to customer needs by Thermo Fisher Scientific has led to the creation of an unrivalled portfolio of IC columns that provides solutions to tackle even the most demanding chromatographic challenges.

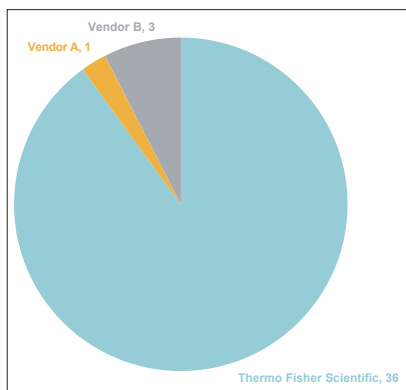


Figure 7. Number of IC column patents issued; comparison by vendor (based on Questel Orbit Intelligence patent search tool).

References

1. H. Small, "Landmarks in the evolution of ion chromatography", *LCGC* **31** (4), 8–15 (2013).
2. C. Pohl, "Recent developments in ion-exchange columns for ion chromatography", *LCGC* **31** (4), 16–22 (2013).
3. M. Verma and C. Tanner, *Benefits of Using 4 µm Particle-Size Columns*. Thermo Scientific White Paper 70631 (2013). <https://assets.thermofisher.com/TFS-Assets/CMD/Reference-Materials/wp-70631-4-micrometer-columns-wp70631-en.pdf>
4. J. Weiss, *Handbook of Ion Chromatography*. Wiley-VCH, Weinheim, Germany (2016). <https://doi.org/10.1002/9783527651610>
5. *Thermo Scientific Dionex IonPac IC Column Selection Guide* (2019). <https://assets.thermofisher.com/TFS-Assets/CMD/brochures/st-70588-ic-column-selection-guide-st70588-en.pdf>
6. U.S. Environmental Protection Agency, *Method 557, Determination of Haloacetic Acids, Bromate, and Dalapon in Drinking Water by Ion Chromatography Electrospray Ionization Tandem Mass Spectrometry (IC-ESI-MS/MS)*, Rev 1.0, 2009
7. *Fast Determination of Haloacetic Acids in Drinking Water*. Thermo Scientific White Paper 72958 (2019). <https://assets.thermofisher.com/TFS-Assets/CMD/Reference-Materials/wp-72958-haloacetic-acids-drinking-water-wp72958-en.pdf>
8. W. Worawirunwong, S.P. Pumkiat and J. Rohrer, *Determination of Cations and Amines in Hydrogen Peroxide by Ion Chromatography Using a RFIC (Reagent-Free) System*. Thermo Scientific Application Update 155 (2017). <http://assets.thermofisher.com/TFS-Assets/CMD/Application-Notes/au-155-ic-cations-amines-hydrogen-peroxide-au72541-en.pdf>
9. H. Small, T.S. Stevens and W.C. Bauman, "Novel ion exchange chromatographic method using conductimetric detection", *Anal. Chem.* **47**(11), 1801–1809 (1975). <https://doi.org/10.1021/ac60361a017>

Ion chromatography is one of the most widely used separation techniques of analytical chemistry with applications in fields such as medicinal chemistry, water chemistry and materials science.

Written by Dr Joachim Weiss, PhD, Technical Director for Dionex Products at Thermo Fisher Scientific, *Basics of Ion Chromatography* is a 265-page ebook which provides a comprehensive introduction to IC. Download your free copy of *Basics of Ion Chromatography* by visiting the link or scanning the QR code.

<https://www.thermofisher.com/BasicsIC-eBook>

About the author

Dr Weiss is recognised as an international expert in analytical chemistry, and the 4th Edition of his *Handbook of Ion Chromatography* was published in 2016. In 2015, he was awarded the Maria Skłodowska Curie Medal of the Polish Chemical Society for his achievements in separation science.



Weights or measures for better calibration

Antony N. Davies^a and Henk-Jan van Manen^{b,c}

^aSERC, Sustainable Environment Research Centre, Faculty of Computing, Engineering and Science, University of South Wales, UK

^bExpert Capability Group – Measurement and Analytical Science, Nouryon Chemicals BV, Deventer, the Netherlands.

<https://www.nouryon.com/company/innovation/eccd/>

^cRadboud University, Institute for Molecules and Materials, Department of Analytical Chemistry & Chemometrics, Heyendaalseweg 135, 6525 AJ Nijmegen, The Netherlands

In traditional approaches to quantitative analysis we teach that the weight is mightier than the volume. You are far more accurate and precise when weighing chemicals to make up standard solutions than using volumetric techniques. There has been some debate about whether this approach carries over into process analytical spectroscopy and other areas of application, where often analyses are of liquid mixtures.

In fact, this column is also something of an apology to all my students who have suffered my sarcasm when they have ever tried to defend the use of volumetric methods over gravimetric to get the best calibration results! It is such a natural reaction that to come up with another view on the world during discussions with Henk-Jan van Manen has been quite refreshing if, looking at my own behaviour, a little worrying.

We are spectroscopists so we all live by Beer's Law—right?

Henk-Jan pointed to an article written by Howard Mark and a number of his colleagues in *Applied Spectroscopy* back in 2010.¹ This paper looked into problems and discrepancies arising using standard gravimetric methods and weight fractions in calibrations for spectroscopic quantitative analysis. Howard Mark has been a prolific writer in the USA over the years, both in the peer reviewed literature and in generating a long series of general interest educational articles with a strong focus on chemometrics in a

similar vein to our own former column editor Tony (A.M.C.) Davies.

For normal quantitative work we all live by Beer's law. Essentially, for each component in our sample, for example in a standard sample cell, there is a linear relationship between their contribution to the overall absorbance signal measured, the specific absorptivity of each component, the concentration of that component and the total pathlength light must travel through the sample. Assuming no changing interactions between the components at different relative concentrations, the pathlength is a constant and a straight-line calibration graph should

This is timely as it has just been announced that Howard and a long-time co-author Jerry Workman Jr have been awarded the 2020 Gold Medal Award by the New York section of the Society for Applied Spectroscopy for their work. Even in COVID-19 times you can get to hear Howard and Jerry speak at the upcoming virtual Eastern Analytical Symposium (EAS). Usually a massive event for analysts with a heavy focus on spectroscopy, this year's online version will be broadcasting sessions live as well as making some presentations available on-demand. Howard and Jerry will both give live presentations on Wednesday 18 November following the presentation ceremony should you wish to attend (free to students registering with their student ID!).²

be obtained for each component, the slope of which depends on how absorbing each individual component is. For the more detailed official IUPAC definition, see Reference 3. Essentially, this underlying linear relationship between concentration and signal is the bedrock of the majority of quantitative spectroscopy. It is normal practice to accept that Beer's law holds true for only dilute systems and that at high analyte concentrations non-linear effects start to adversely affect quantitative analysis studies.

Weight fractions or volume fractions—that is the question?

So what Howard Mark observed in his original paper was the lack of clear understanding of the impact that selecting a particular way of expressing "concentration" might have on the use of chemometric models, particularly when applied to mixtures of liquids, which are commonly found in industrial applications of vibrational spectroscopy. The most widely used weight% concentration unit in analytical spectroscopy was challenged in his paper in a logical way. He showed the linear relationship between volume% and concentration using near infrared (NIR) spectroscopy and drawing on the observation that for pure liquids there is not a clear linear relationship between weight% and volume% for liquids of different densities (he originally reported data for binary and ternary mixtures of toluene, dichloromethane and *n*-heptane). Figure 1 shows spectroscopic

TONY DAVIES COLUMN

experimental results from the Deventer team using CLS on 21 binary mixture spectra as done by Howard Mark. This emphasised the potential deviation from the accepted Beer's law linear relationship between "concentration" and signal intensity if mass or volume fractions are used.

Kim Esbensen, Paul Geladi and Anders Larsen followed up in 2012 with a nice short article in *NIR news* in their "Mythbusters in Chemometrics" column which reinforced Howard's observations.⁴ They studied data provided to them on 70 mixtures of five components (butanol, dichloromethane, methanol, dichloropropane and acetone). Their article includes two figures (Figure 2 for butanol and Figure 3 for methanol), which were quite startling to my eyes as they showed an effect I have seen regularly in chemometric calibrations, but which I had put down to, maybe wrongly, inaccuracies in the reference method concentration determinations.

In 2017, Howard published another article on this topic in *NIR news* directly looking at the effect of the selection of the measurement units on NIR calibrations.⁵ In this article he focussed more on common effects observed in NIR chemometric models and how the impact of selecting mass fraction rather than volume can impact the quality of the results. The difference between using Classical Least Squares (CLS) algorithms and Partial Least Squares (PLS) and other models is highlighted (see below).

However, to muddy the waters a little, a paper was published recently by Yan

and co-workers which reported that they had been unable to confirm the benefit of using volume% over weight% concentration units in their studies of benzene/cyclohexane/ethylbenzene and ethyl acetate/heptan-1-ol/1,4-dioxane ternary mixtures.⁶ Although they were looking primarily for the effect of hydrogen bonding on the performance of CLS and PLS algorithms.

Have sympathy on the overworked chemometric algorithms!

Howard selected CLS for his study, partly because it is the easiest chemometric model to explain, consisting essentially of linear combinations of pure component spectra to make up the overall observed spectrum. The drawback is that you are assuming no interactions between the components in the mixture, such as were studied by Yan and co-workers. Howard and others have remarked that the inability of CLS models to cope with other types of interactions is one of the reasons PLS and other models tend to be favoured (including by the authors of this column, as I have mentioned in previous articles). PLS modelling can often be accused of overfitting, as more factors are used to create the model than you would think are really necessary—and one conclusion could well be that the PLS algorithm (essential a model expecting a linear relationship between concentration and signal) is having to work overtime to cope with the fact that the concentration data it is being fed is not actually strictly linear.

The model, therefore, is often generated with additional factors to try to compensate for this non-linearity.

So how bad can it get? Well, the papers cited claim that the non-linearity can cause errors in the calibrations of up to 10–15%. So, this is one of the reasons that Henk-Jan and his team from Nouryon and the Radboud University in Nijmegen decided to get a definitive answer to the question of weight against volume, as 10–15% wrong in an industrial control process could be worth a lot of money!

Robotics for more reproducible calibration samples

One of the aspects of ensuring good quality analytical measurements is acknowledging and minimising errors from sources that might obscure the changes in the data you are analysing. The Royal Society of Chemistry Analytical Methods Committee of the Analytical Division produce good Technical Briefs to help analytical chemists and they identify human error as the greatest source of problems during chemical analysis.⁷ Henk-Jan's team required the best possible accuracy and precision in their production and measurement of the various binary solvent mixtures they were investigating. As human error in weighing and mixing samples both by individuals and between different experimenters can introduce noise, it was decided to exploit a suite of robots available for use in projects at the Expert Capability Center Deventer.⁸ They used a high-throughput liquid handling robot from Syntegon Technology GmbH (formerly known as Bosch Packaging Technology) to prepare their binary liquid systems with 30 samples being prepared across the full mass or volume fraction range from 0 to 1 (Figure 2). They also have access to a repurposed high-throughput Lipos robotic platform (Zinsser Analytic GmbH, Frankfurt, Germany) which was set up to allow automated spectroscopic determinations of the samples (Figure 3). This robot was equipped with online NIR measurements performed on a Bruker MPA instrument (Bruker Optics, Ettlingen, Germany), Raman measurements using a Kaiser RXN-4 instrument

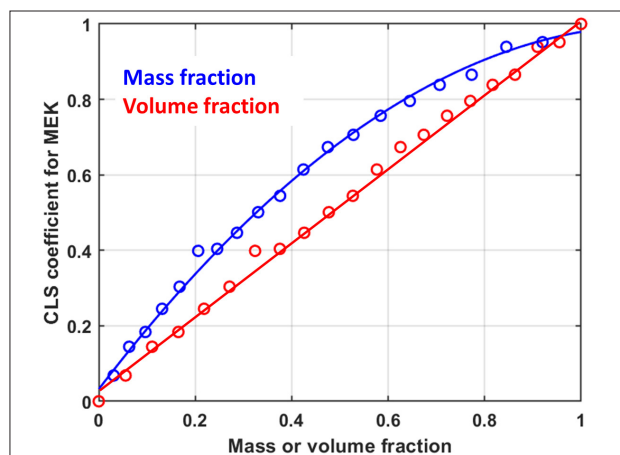


Figure 1. Comparison between the NIR spectroscopic signal of a binary mixture of chloroform/MEK (methyl ethyl ketone).

TONY DAVIES COLUMN

(Kaiser Optical Systems, Ann Arbor, MI) by using a fibre-optic probe and further supported by mid-infrared spectroscopic measurements using a Spectrum 100 instrument (PerkinElmer, Groningen, The Netherlands) in attenuated total reflection mode using a diamond crystal (Figure 3).

Henk-Jan and the team deliberately selected binary systems of pure liquids, avoiding materials that might suffer from strong inter-component interactions when mixed. They chose chloroform/heptane, chloroform/toluene, toluene/heptane and methylethylketone (MEK)/heptane. And, unfortunately, that is all we are going to say about their study to confirm Howard Mark's original observations for now... you will have to wait until the full paper is published to get at all the juicy details!

Conclusions

What these various pieces of work over the last 10 years show, apart from the fact that I need to be kinder to my students, is that we need to always bear in mind whether handed-down wisdom should be accepted as-is or be challenged when we start to see effects that we cannot easily explain.

I have always hated being reliant on "black-box" approaches to achieving analytical results, which used to be propagated by some chemometricians. I often annoy colleagues by persistently asking "but why?" like a petulant child when getting answers such as "we don't know", "we just ignore that", "just trust the algorithm". Howard Mark's work and the subsequent studies have at least provided some answers to effects we

see in everyday experiments which are unexpected.

Henk-Jan's teams' confirmatory experiments and results will be published elsewhere in full, when we have the link, we will add it to the online version of this column. Everyone please, stay safe!

Acknowledgements

HJM would like to thank Nouryon colleagues Jan Gerretzen, Martijn Smout, Ali Ghamati and René van Egdom and Radboud colleagues Geert Postma and Jeroen Jansen.

References

1. H. Mark, R. Rubinovitz, D. Heaps, P. Gemperline and D. Dahm, "Comparison of the use of volume fractions with other measures of concentration for quantitative spectroscopic calibration using the classical least squares method", *Appl Spectrosc.* **64(9)**, 995–1006 (2010). <https://doi.org/10.1366/000370210792434314>
2. <https://eas.org/2020/>
3. <https://goldbook.iupac.org/terms/view/B00626>
4. K.H. Esbensen, P. Geladi and A. Larsen, "'Concentration' is a fixed, immutable property", *NIR news* **23(5)**, 16–18 (2012). <https://doi.org/10.1255/nim.1317>
5. H. Mark, "Effect of measurement units on NIR calibrations", *NIR news* **28(3)**, 7–11 (2017). <https://doi.org/10.1177/0960336017703255>
6. H. Yan, Y. Ma, Z. Xiong, H.W. Siesler, L. Qi and G. Zhang, "Quantitative analysis of organic liquid three-component systems: near-infrared transmission versus Raman spectroscopy, partial least squares versus classical least squares regression evaluation and volume versus weight percent concentration units", *Molecules* **24(19)**, 3564 (2019). <https://doi.org/10.3390/molecules24193564>
7. Analytical Methods Committee, AMCTB No 56, "What causes most errors in chemical analysis?", *Anal. Meth.* **5**, 2914–2915 (2013). <https://doi.org/10.1039/C3AY90035E>
8. <https://www.nouryon.com/company/innovation/eccd/>

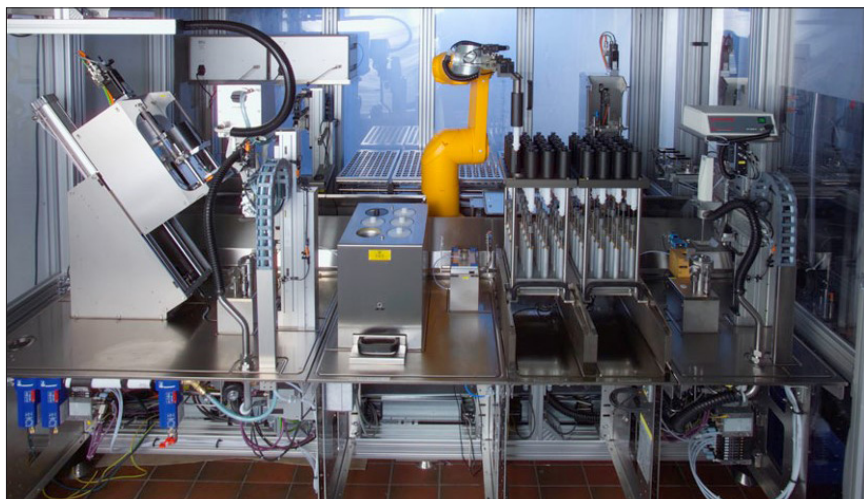


Figure 2. High-throughput liquid handling robot from Syntegon Technology GmbH used for reference liquid sample preparation to reduce error in the reference mixture preparation.

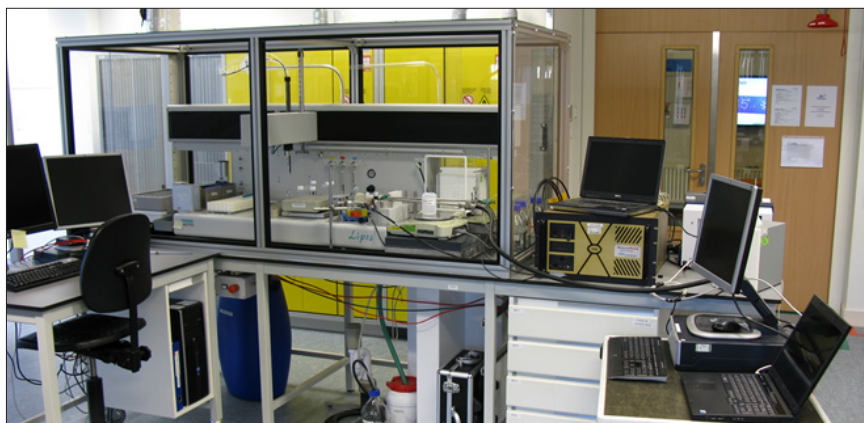


Figure 3. Zinsser robot at the Expert Capability Center in Deventer with integrated automatic spectroscopic analysis of the liquid samples created by the other high-throughput liquid handling robot.

Chemical analysis of contaminated soil for sound environmental site assessment. Part 2

Jean-Sébastien Dubé, ing. PhD and François Duhaime, ing. PhD

Laboratoire de géotechnique et génie géo-environnemental, Département de génie de la construction, École de technologie supérieure, 1100 Notre-Dame ouest, Montréal (QC), Canada H3C 1K3

Proper sampling of particulate matter for instrumental analysis is a common task in many applied scientific, technology and engineering fields. It is a crucial task for ensuring that measurements made on a given set of samples are representative estimate of the parameters of interest in the original sampling target. Unfortunately, sampling particulate matter is, in many fields, performed without a scientific basis, mostly because its critical role is ignored, or at best, misunderstood, and because of an unawareness of, sometimes a disregard for, the Theory of Sampling. This second part compares grab sampling with composite sampling further illustrating this important issue, again using experience in the field of geo-environmental engineering.

Fix your sampling, not your results

In this second part, we illustrate how measurement variability can be controlled at the sampling stage with a real-world example from a recent study conducted at École de Technologie Supérieure (ETS), Montréal, in partnership with the same consultant involved in the studies presented in the first Part. In this study, we compare the uncertainty derived from grab sampling to that derived from a Theory of Sampling (TOS)-compliant composite sampling process. We here use unpublished results to illustrate a critical distinction which has universal implications: namely that between subjective, purposive or haphazard sampling (i.e. grab sampling) and probabilistic, TOS-compliant composite sampling.

Figure 1 shows lead (Pb) concentration measurements made on samples from a given sampling location in a specific soil parcel using these two fundamentally opposing sampling approaches.

By using an experimental design, each approach resulted in several analytical samples in order to assess the various uncertainties involved, sampling vs analytical.

The composite sampling approach unavoidably resulted in larger masses for the primary field samples, which demanded appropriate sub-sampling techniques (in the field or in the laboratory) on the way towards the analytical aliquot. These mass-reduction procedures, and the equipment used, are

specifically designed for reducing and eliminating sub-sampling errors. Grab sampling on the other hand does not allow any control on sampling errors. In our study, grab sampling was performed by the consultant company following “usual sampling procedures”. The reader is referred to Boudreault *et al.*¹ for more



Figure 1. Left: excavated soil at a sampling station. The soil is placed in a longitudinal pile and corresponds to an identifiable layer of a given material (based on visual observation), or to a 50 cm (at most) layer if visual differentiation was not possible. Right: vertical increments are taken perpendicular to the longitudinal axis of the pile and over its total height. The primary sample mass obtained in this manner was approximately 13 kg of dry matter.

SAMPLING COLUMN

details on the project, to Gy,²⁻⁴ Pitard⁵ and Esbensen⁶ for more on the TOS, and to Gerlach *et al.*^{7,8} and Petersen *et al.*⁹ for more on mass reduction techniques.

Figure 4 illustrates the risks incurred with grab sampling, as also evidenced in the first example above. In practice, only one concentration measurement would have been made and used for decision-making regarding the disposal of this soil parcel. As in the first example, it is still impossible to categorise this soil parcel with any certainty. On the other hand, the TOS-compliant composite sampling procedure yielded much better results—

indeed all measurements fall in the *same* contamination level category. In fact, any of these measurements could have been used to categorise the soil and make a correct decision regarding the fate of this soil parcel.

Appropriate reflections in geo-environmental engineering

To what lengths should one go to improve sampling procedures before analysis? This question will often be asked by consultants or soil analysts faced with poor results stemming from

incorrect sampling. It is a legitimate question, as changes to the sampling process will reflect on the perceived efficiency of their current operations, performances and reliability.

In the present example, the composite primary sampling required six mass reduction and two comminution steps to obtain an analytical sample, *compared* to only two mass reduction steps in grab sampling. But, as is clear, ease-of-performance comes at a fatally inflated Total Sampling + Analytical Errors (TSE + TAE), which is never worth risking when lot heterogeneity is significant.

For conciseness, this column will only address the first consideration of any compound sampling operation, the field sampling. The goal is to ensure that all types of particles have a uniform, non-zero probability of being sampled, i.e. compliance with the Fundamental Sampling Principle (FSP).

But things are not necessarily easy in geo-environmental engineering. What is a particle? What differentiates one particle from another? In the TOS, this is described by the constitutional heterogeneity of the soil, which reflects the size and shape of the particles as well as their composition and density. When sampling contaminated soil, for instance, particles can be of *geogenic* or *anthropogenic* origin, or *both*. Thus in general there may be matrix (soil) particles, contaminant particles, as well as matrix particles *coated* with contaminants. Such a constitutional heterogeneity is complex and difficult to describe in simple mathematical terms. However, to ensure that each of these types of particles is present at each sampling stage during the sampling process, Pitard⁵ states that “the first rule to fulfil is to ensure that the sample is representative of **all** the **particle size fractions**”. Of course the TOS, and Pitard, emphasise that this objective also depends on particle density, but, here Pitard at least provides us with a reasonable starting point. However, even on this basis, geo-engineering encounters problems.

In many fields it is not uncommon for analytical protocols to require that a sample should only have particles smaller than 2 mm, thus leading



Figure 2. Primary samples obtained from the piles shown in Figure 1, which were reduced in the field using fractional shovelling as shown. Each fraction correspond to a final field sample sent to the laboratory. Secondary sample mass thus obtained was approximately 600 g of dry matter.



Figure 3. Left: close-ups of a sample from field fractional shovelling (Figure 2). These samples were brought to the laboratory where they were air-dried and ground (milled) before a first mass-reduction using sectorial rotary splitting (SRS). In the left picture, the maximum particle size is approximately 2 cm. Right: these samples were then milled and ground further before a final SRS step to obtain analytical samples of approximately 1 g of dry matter. In the right picture, the maximum particle size is approximately 200 μm .

SAMPLING COLUMN

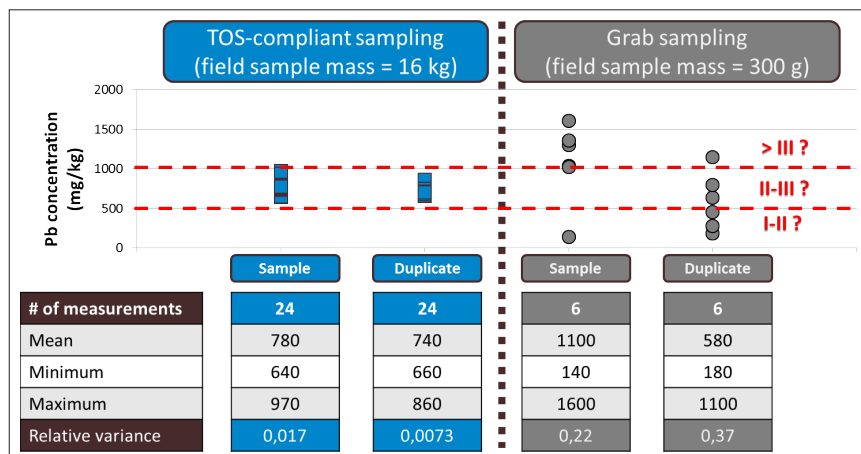


Figure 4. Comparison of uncertainty between TOS-compliant composite sampling and grab sampling based on the effective TSE + TAE. The average relative variances correspond to coefficients of variation of 11% and 54% for composite and grab sampling, respectively. There is no doubt which approach is the only acceptable approach for reducing the dominant field sampling errors.

to the analyst to subjectively remove larger particles, or to *screening* the sample with a sieve with the appropriate screen size threshold. If the particle size distribution of samples is *altered* before analysis, the risk of biasing the results is significant.^{5,6} A crucial aspect of preserving the representativeness of size fractions is identifying the so-called *critical size fraction*, i.e. the size fraction of high(est) interest—which often also has the highest impact on the heterogeneity (but not always). This target corresponds to the largest particle size(s) in which the analyte is to be found.

However, too often, current sampling guidelines require the *arbitrary* removal of all large particles under the hypothesis that the smaller particles represent a greater risk to public health. This may, or may not, be true—far from automatically in all cases.

Thus, on contaminated sites, contaminants are also found in large particles of anthropogenic origin, e.g. clinker, slag or associated with particle coatings. Great care must be taken in identifying the critical size fraction for each case individually, since this will determine the minimum sample mass needed to ensure representativeness of particles of equal size, or smaller, than the critical size fraction. This issue is discussed in much more detail in Dubé *et al.*¹⁰

Current geo-environmental guidelines and standards

Geo-environmental engineers and scientists tasked with environmental site assessment currently only have a few cardinal resources for determining minimum sample mass and for selecting appropriate mass reduction techniques. One such leading resource is ASTM Standard D6913 for the determination of the particle-size distribution (PSD) by sieve analysis and its accompanying standard practice C702. D6913 recommends minimum sample mass requirements based on maximum particle size and the number of significant digits for reporting PSD results.

We have previously discussed that the minimum sample mass requirements in D6913 are **not** compliant with TOS principles, but rather defer to practical requirements to avoid sieve overloading or for composite sieving. And also D6913 fails to address the constitutional heterogeneity of the soil and the critical size fraction properly, but rather seeks to adapt the sampling process to existing equipment, which obviously will fail. Therefore, the minimum mass requirements in D6913 actually lead to significantly *larger* variability in analytical results than expected.¹⁰

ASTM D6913 and C702 also prescribe the use of mass reduction techniques for the procurement of the sample for

traditional analysis. Riffle splitting (RS) is recommended for dry flowing soil, while coning and quartering (C&Q) and miniature stockpile sampling (MSS) are suggested for moist soil. However, D6913 and C702 do not justify these recommendations based on performance data or any other evidence. Analysing their performance and comparing them for their recommended use, i.e. RS for dry soil versus C&Q and MSS for moist soil, may also be misleading. For moist soil, sampling variability significantly decreases due to matrix moisture and increased coherence and hence reduced segregation.¹⁰ Therefore, a sampling method which performs apparently well on moist material, could perform very poorly on dry material. Petersen *et al.*⁹ have observed that splitting methods outperformed shovelling methods for dry materials. Moreover, Pitard⁵ and Esbensen⁶ strongly advise against the use of coning and quartering and miniature stockpile sampling (also called degenerate fractional shovelling).

Discussion and conclusions

The present exposé, Parts 1 and 2, focuses on how incorrect primary and secondary sampling can severely affect the quality and validity of analytical measurements made on the resulting aliquots. The context of soil sampling in environmental site assessment was used to illustrate several critical issues related to practical sampling before analysis. We have also emphasised that all size fractions in the sampled particulate matter must be proportionally present in any sample thereof, lest all hopes for representativity be lost.

It was seen that it is not a straightforward matter simply to rely on current guidelines and standards. Most, sadly, ignore the TOS, at their peril, and even provide recommendations which *violate* its principles. Unknowingly, the analyst will then make measurements on samples which are not representative of the initial lot to be characterised.

Because of such general lack of awareness of the TOS, it is also difficult for analysts to understand their role with respect to the representativeness of the

Introduction to the Theory and Practice of Sampling

Kim H. Esbensen

with contributions from Claas Wagner, Pentti Minkkinen, Claudia Paoletti, Karin Engström, Martin Lischka and Jørgen Riis Pedersen

“Sampling is not gambling”. Analytical results forming the basis for decision making in science, technology, industry and society must be relevant, valid and reliable. However, analytical results cannot be detached from the specific conditions under which they originated. Sampling comes to the fore as a critical success factor before analysis, which should only be made on documented representative samples. There is a complex and challenging pathway from heterogeneous materials in “lots” such as satchels, bags, drums, vessels, truck loads, railroad cars, shiploads, stockpiles (in the kg–ton range) to the miniscule laboratory aliquot (in the g– μ g range), which is what is actually analysed.

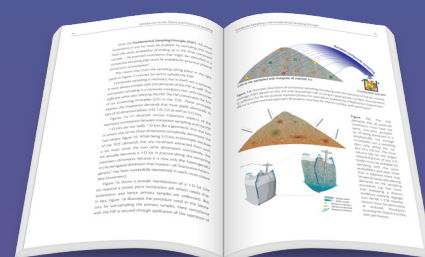
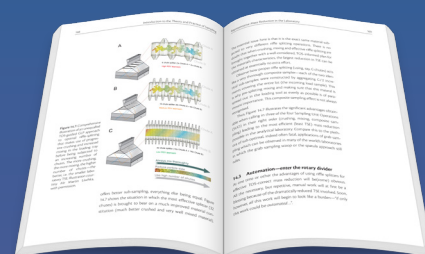
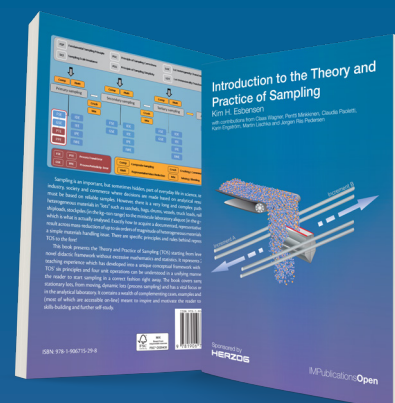
This book presents the Theory and Practice of Sampling (TOS) starting from level zero in a novel didactic framework without excessive mathematics and statistics. The book covers sampling from stationary lots, from moving, dynamic lots (process sampling) and has a vital focus on sampling in the analytical laboratory.

“I recommend this book to all newcomers to TOS”

“This book may well end up being the standard introduction sourcebook for representative sampling.”

“One of the book’s major advantages is the lavish use of carefully designed didactic diagrams”

NEW
BOOK



impopen.com/sampling

MPublicationsOpen

SAMPLING COLUMN

Factbox

Below, we present performance results for the mass reduction methods recommended by D6913/C702 and compare them to fractional shovelling and grab sampling. ASTM 6913 only recommends RS for dry soil, but for reasons discussed

above, all methods were compared using only dry soil here.

Figure 5 shows the expanded uncertainty ($k=3$) for the particle size distribution (PSD) obtained for each method on the *same soil*. As expected, RS performs better than the other shovelling-based methods. Amongst the latter, fractional

shovelling performs better than C&Q, while MSS is approximately equivalent to grab sampling and thus performs almost as poorly.

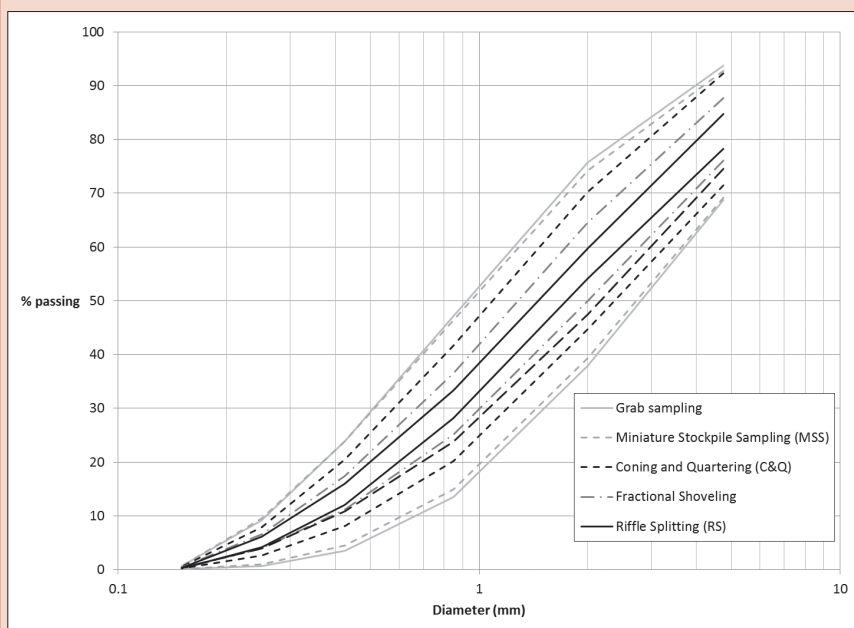


Figure 5. PSDs of a comparison soil obtained using three sampling techniques recommended in ASTM 6913 (MSS, C&Q, RS), fractional shovelling and grab sampling.



Figure 6. Soil corresponding to the PSD results shown in Figure 5. The laboratory bench pile shows a distinct constitutional and size heterogeneity manifestation. In this picture, it was undergoing sampling using MSS as defined in ASTM D6913. Samples were obtained by combining three increments grabbed from subjectively selected spots on the pile. The resulting sub-samples are seen in the metal plates in the top-right corner.

measurement data. Their focus is largely on the final measurements in the laboratory, but their work manifestly includes sub-sampling to reduce the mass of particulate matter so as to comply with the inherent volume/mass requirements of the analytical instrumentation. In environmental site assessment, analysts are *de facto* an essential part of the whole “from-lot-to-aliquot” pathway, as they at least perform the necessary last mass reduction, which represents a minimum of two orders of magnitude of mass reduction—and which at times often also involve a highly subjective removal of “larger particles”.

The first parts of the full sampling-and-analysis process occur in the field and are often performed by the consultant’s field technician. This gap in the “chain of custody” of the sampling process

between the consultant and the laboratory is particularly problematic, especially as much as the current incorrect sampling practices are left without a clear responsibility. No one takes full responsibility for the representativeness of the *complete* sampling process in such circumstances. A possible solution would be that a single responsible *agent*, knowledgeable in the TOS, should design, perform and ultimately be responsible for the *whole* sampling process until analysis. Analysts would then only receive representative test portions, aliquots, ready for analysis and would, therefore, be able to fully take responsibility for the quality of their measurements, i.e. the true TAE, while the responsibility for quantifying all sampling and sub-sampling uncertainties *before* the analytical aliquot (TSE) would also have been clearly described and assigned.

Technically, the conclusion from the above two, out of *many* similar studies, is that composite sampling at the primary sampling stage is *imperative* and should be *mandatory* for all significantly heterogeneous materials that cannot be subject to mixing. The necessary additional crushing and sub-sampling stages, which will vary significantly as a direct consequence of the material heterogeneity encountered, are simply the price to pay for documentable primary sample representativity without which the *raison d’être* of analysis has disappeared: what could be the reason for analysing a sample (or a derived aliquot) that is known to be non-representative? None. There is no such reason.

There are no shortcuts to representative sampling! Composite sampling must always be used, as this is the only avail-

SAMPLING COLUMN

able guarantee for representativity of significantly heterogeneous materials. Contaminated soil is an excellent basis upon which to demonstrate these essential truths because of its often dramatically complex nature.

Acknowledgements

The authors thank Jean-Philippe Boudreault and Laurent Nolak.

References

1. J.-P. Boudreault, J.-S. Dubé, M. Sona and É. Hardy, "Analysis of procedures for sampling contaminated soil using Gy's Sampling Theory and Practice", *Sci. Total Environ.* **425**, 199–207 (2012). <https://doi.org/10.1016/j.scitotenv.2012.03.013>
2. P. Gy, "Sampling of discrete materials—a new introduction to the theory of sampling I. Qualitative approach", *Chemometr. Intell. Lab. Syst.* **74**, 7–24 (2004) <https://doi.org/10.1016/j.chemo-lab.2004.05.012>
3. P. Gy, "Sampling of discrete materials II. Quantitative approach—sampling of zero-dimensional objects", *Chemometr. Intell. Lab. Syst.* **74**, 25–38 (2004) <https://doi.org/10.1016/j.chemo-lab.2004.05.015>
4. P. Gy, "Sampling of discrete materials III. Quantitative approach—sampling of one-dimensional objects", *Chemometr. Intell. Lab. Syst.* **74**, 39–47 (2004) <https://doi.org/10.1016/j.chemo-lab.2004.05.011>
5. F.F. Pitard, *Theory of Sampling and Sampling Practice*, 3rd Edn. CRC Press, Taylor & Francis Group (2019). <https://doi.org/10.1201/9781351105934>
6. K.H. Esbensen, *Introduction to the Theory and Practice of Sampling*. IM Publications Open (2020). <https://doi.org/10.1255/978-1-906715-29-8>
7. R.W. Gerlach, D.E. Dobb, G.A. Raab and J.M. Nocerino, "Gy sampling theory in environmental studies. 1. Assessing soil splitting protocols", *J. Chemometr.* **16**, 321–328 (2002). <https://doi.org/10.1002/cem.705>
8. R.W. Gerlach, J.M. Nocerino, C.A. Ramsey and B.C. Venner, "Gy sampling theory in environmental studies: 2. Subsampling error estimates", *Anal. Chim. Acta* **490**(1–2), 159–168 (2003). [https://doi.org/10.1016/S0003-2670\(03\)00568-3](https://doi.org/10.1016/S0003-2670(03)00568-3)
9. L. Petersen, C.K. Dahl and K.H. Esbensen, "Representative mass reduction in sampling—a critical survey of techniques and hardware", *Chemometr. Intell. Lab. Syst.* **74**(1), 95–114 (2004). <https://doi.org/10.1016/j.chemo-lab.2004.03.020>
10. J.-S. Dubé, J. Ternisien, J.-P. Boudreault, F. Duhaime and Y. Éthier, "Variability in particle size distribution due to sampling", *Geotech. Test. J.* **44**(1), 26 (2021). <https://doi.org/10.1520/GTJ20190030>



"...all size fractions in the sampled particulate matter must be proportionally present in any sample thereof, lest all hopes for representativity be lost"

NEW PRODUCTS

IMAGING

Diamond-shaped capillary holder insert adds flexibility to Linkam stage

Linkam Scientific Instruments has added a diamond-shaped capillary holder insert to its CAP500 stage, allowing the temperature control stage to be quickly and easily adapted to hold either of two capillary sizes simply by rotating the capillary holder. The CAP500 stage is designed to study samples in a high pressure quartz capillary, controlling the temperature of a capillary section up to 50 mm in length from $<-195^{\circ}\text{C}$ up to 500°C . Samples can be pumped through the capillary at a specific pressure using a pump and pressure gauge to investigate the flow dynamics and rheology of the sample with respect to temperature and pressure using a range of microscopy and spectroscopic techniques including brightfield, IR, X-ray or Raman.

The capillary is inserted through the body of the chamber and housed in a 1.0 mm \varnothing channel inside a 50 mm silver block. The block itself has been designed and engineered to provide a uniform temperature across the length of the capillary. Capillaries loaded into this channel can be moved 25 mm in the x direction and 3.5 mm in the y direction using the xy mechanism to allow for observation across the length of the sample in the capillary. The standard capillary sizes are 1/8" and 1/16", but customised



diamond-shaped inserts allow for different-sized capillaries with an outer diameter of ≤ 0.6 mm. A Dual Capillary CAP500 option is also available: two capillaries can be mounted side by side, then the CAP500's XY mechanism can be used to move each capillary over the light aperture for imaging.

Linkam Scientific Instruments

► <http://link.spectroscopyasia.com/32-085>

INFRARED

FT-IR hand sanitiser now tests ethanol and isopropanol concentrations

PerkinElmer's Hand Sanitiser Analyser instrument can be used to test for the presence of methanol in alcohol-based hand sanitiser products with pass/fail results delivered in 30s or less. Recent warnings and recalls from the FDA indicate that methanol can be toxic to consumers if absorbed through the skin and life threatening if ingested. The instrument, introduced in April 2020, also tests hand sanitisers for concentration levels of desired alcohols, such as ethanol and isopropanol, to help assure product efficacy per WHO, USP or FDA guidelines.

The compact and portable analyser is based on the Spectrum Two™ FT-IR spectrometer. The underlying technology allows for rapid detection of methanol contamination down to 0.03% (or 300 ppm), which is more sensitive than the FDA-mandated detection limits.

PerkinElmer

► <http://link.spectroscopyasia.com/32-084>

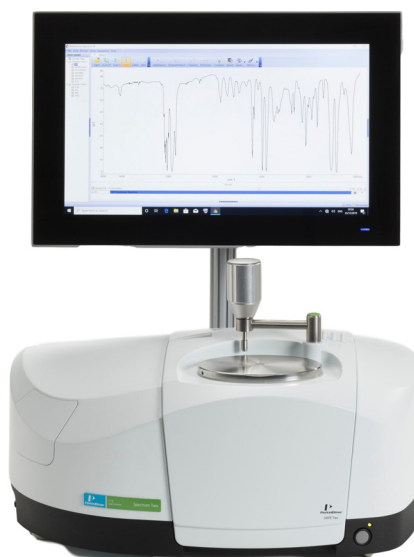
LUMINESCENCE

FLIM imaging with 10-ps time resolution

PicoQuant has developed rapidFLIM^{HiRes} which enables the imaging of samples at up to 15 frames per second with a time resolution of 10 ps using Fluorescence Lifetime Imaging (FLIM). rapidFLIM^{HiRes} provides both rapid data acquisition and high time-resolution when studying fast processes such as protein

interactions, FRET dynamics, ion fluxes or quickly moving species.

The rapidFLIM^{HiRes} approach exploits a series of hardware capabilities recently introduced by PicoQuant to overcome the limitations of classic, Time-Correlated Single Photon Counting (TCSPC) based FLIM: namely hybrid photomultiplier detectors capable of



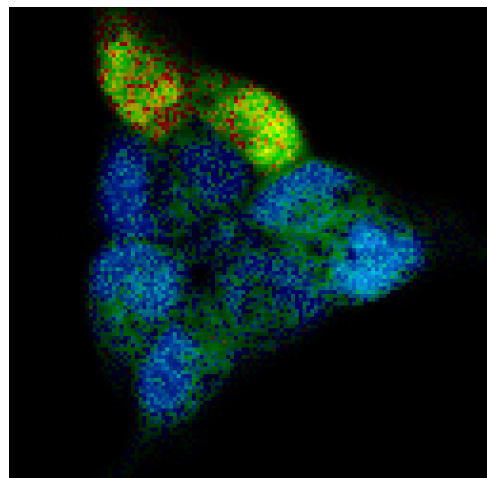
NEW PRODUCTS

handling count rates of about 78 Mcps, the MultiHarp 150 4P TCSPC module with four parallel detection channels, a dead time of 650 ps and time bin widths as small as 10 ps. Furthermore, the SymPhoTime data acquisition and analysis software has been updated with memory management and processing time improvements as well as correction algorithms to reduce decay curve distortions due to very high count rates and artefacts of the detector pulse pile-up. The SymPhoTime 64 software stores all raw photon timing information in the portable TTTR file format, so that no data is lost and can always be analysed with a broad array of commercial and open source tools.

All components required for rapidFLIM^{HiRes} are available either individually, as part of a PicoQuant Laser Scanning Microscopy (LSM) Upgrade Kit for systems from Nikon, Olympus, Scientifica or Zeiss and as a special configuration of PicoQuant's MicroTime 200 confocal time-resolved microscopy platform.

PicoQuant

► <http://link.spectroscopyasia.com/32-088>

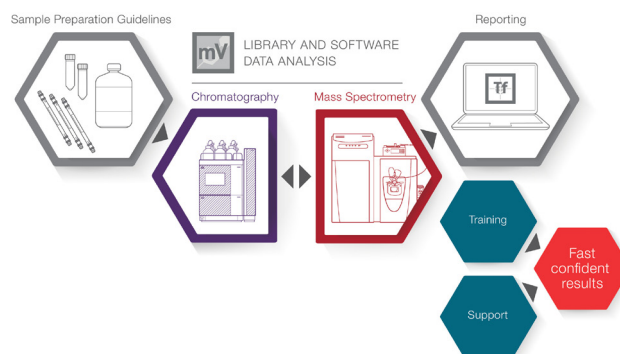


MASS SPECTROMETRY

Toxicology LC-MS workflow

The new Thermo Scientific Tox Explorer Collection offers a comprehensive LC-MS workflow for toxicology assays. The Tox Explorer Collection consists of proven methods enabling toxicology laboratories to achieve accurate, high-resolution data, regardless of analyte type, matrix complexities or user expertise. The Tox Explorer Collection consists of a comprehensive library of analytes, allowing for faster identification and targeted screening assays with 1500 compounds confirmed in a single analysis.

The Thermo Scientific Tox Explorer Collection is composed of the following components: Thermo Scientific Q Exactive Plus Hybrid Quadrupole-Orbitrap mass spectrometer; Thermo Scientific Vanquish Flex UHPLC system; Thermo Scientific TraceFinder software; Thermo Scientific Accucore column and consumables configured for high performance; an extensive HRAM mzVault library of 1500+ compounds and database with streamlined data processing and reporting; proven method comprising critical hardware parameters along with a step-by-



step walkthrough guide for quick start-up and method installation; and application support and training.

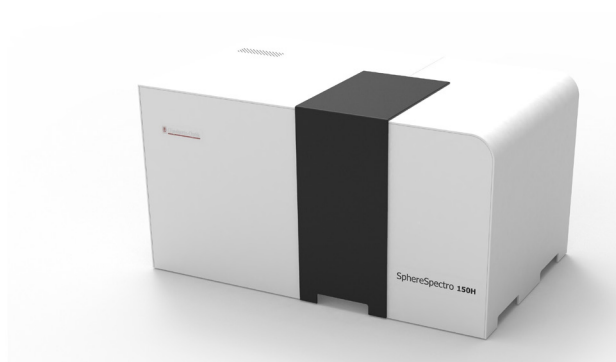
Thermo Fisher Scientific

► <http://link.spectroscopyasia.com/32-089>

NIR

Spectrometer system determines scattering and absorption coefficients of turbid media

Gigahertz-Optik's SphereSpectro 150H spectrometer system enables the simultaneous determination of the spectral absorption and scattering coefficients for scattering samples. The sample is illuminated and the transmitted as well as the reflected light is measured and evaluated in a differentiated manner using radiative transfer theory. For clear samples, the absorption coefficient is determined based on Beer-Lambert's law. However, if the sample exhibits scattering (i.e. turbid or translucent samples),



NEW PRODUCTS

the entire physical process must be taken into account, i.e. a combination of scattering and absorption properties.

The determined absorption coefficient is identical to the absorption coefficient determined conventionally for clear media and can be used for content determinations, for example. The SphereSpectro 150H uses an integrating sphere to measure the total reflected and transmitted light of an illuminated sample. From these two quantities, the absorption coefficient and the effective scattering coefficient can be calculated.

Broadband NIR LED for spectroscopy applications

The Osram P1616 SFH 4737 from Osram measures $1.6 \times 1.6 \times 0.9$ mm, and is only half the size of the previous smallest product in the Osram portfolio. This compact design makes it suitable for use in smartphones, as well as its output of 74 mW at 350 mA, which is about three times the peak values of earlier solutions. It also has radiant intensity in the forward direction at 18 mWsr^{-1} , which is double those of former Osram NIREDS. Its wavelength range is 650–1050 nm. The sensitivity

The SphereSpectro 150H covers the wavelength range between 200 nm and 2150 nm. Modular versions are also available for sub-ranges within this spectral range. The spectrometer also benefits from simple operation, short measurement times and a large sample chamber with optimised sample holder.

Gigahertz-Optik

► <http://link.spectroscopyasia.com/32-086>

of legacy silicon-based detectors usually decreases with increasing wavelength, especially above 950 nm. In the past, in order to compensate for this, higher currents were required. Thanks to a new phosphor, the component emits more light at higher wavelengths—with positive effects on the overall energy consumption of the system.

Osram

► <http://link.spectroscopyasia.com/32-090>

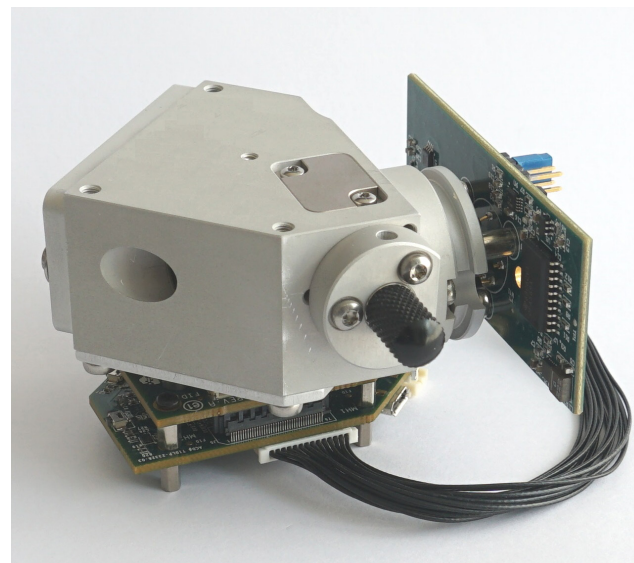
PEAK XNIR spectrometer with DLP® technology from Ibsen Photonics

Ibsen Photonics has released the new PEAK XNIR OEM spectrometer that features DLP® Pico™ technology from Texas Instruments. The PEAK XNIR offers high throughput due to a retroreflective optical design, a high efficiency transmission grating and a NA of 0.22. The retroreflective design allows for a compact form factor of approximately $63 \times 50 \times 77$ mm with high resolution and sensitivity as well as environmental ruggedness. The wavelength range is 1650–2400 nm and the resolution is 10 nm.

The PEAK XNIR is supplied with control electronics and uses Ibsen's XNIR Evaluation Software for Windows with advanced column and Hadamard scan functions for improved signal-to-noise ratio. You can program your own software using an HDI standard interface and read/write operations to the FPGA register. PEAK utilises Ibsen's high efficiency fused silica transmission gratings combined with the DLP technology from Texas Instruments in order to provide the spectral programmability. Another benefit of using Ibsen's transmission gratings is that PEAK can be manufactured in high quantities with very small unit-to-unit performance variation.

Ibsen Photonics

► <http://link.spectroscopyasia.com/32-091>



UV/VIS

UVC radiometer for germicidal UV sources

The new X1-1-UV-3727 radiometer from Gigahertz-Optik is designed to accurately measure the far-UVC irradiance or dose produced by 222-nm excimer lamps. This is in addition to the measurement of other germicidal UV source types including low pressure Hg lamps and UV LEDs. Each meter has a wide dynamic range and is supplied with a traceable calibration certificate. Far-UVC radiation, such as the 222 nm produced by Kr-Cl exci-

mer lamps, has been the subject of many studies and is known to be effective against a wide range of pathogens. Significantly, it is also thought to offer less photobiological hazard, because far-UVC light cannot penetrate human skin as deeply as the longer wavelength UV radiation produced by low pressure Hg lamps and UVC LEDs.

Gigahertz-Optik

► <http://link.spectroscopyasia.com/32-087>

Use this page to register for a free subscription to *Spectroscopy Asia*. You can also register online at the address below.

Online version at <http://www.spectroscopyasia.com/register>

1. Your Details

Title (Professor/Dr etc.):	First Name:	Last Name:
Organisation Name:	Address:	
City:	Postal Code:	State/Region:
Country:	Job Title:	

Please send me/continue to send me a free copy of *Spectroscopy Asia*.

Signed: _____ E-mail: _____

Date: _____

Field of Work:

(please tick ALL that apply)

- Agriculture
- Biotechnology
- Chemicals
- Cultural Heritage
- Electronics/Semiconductors
- Energy and Fuels
- Environment
- Food
- General Analysis
- Instrumentation
- Life Science
- Materials Science
- Medical Sciences
- Metals and Minerals
- Nanotechnology
- Pharmaceuticals
- Proteomics and other -omics
- Polymers and Peptides
- Security and Forensics
- Water

Techniques:

(please tick ALL that apply)

- Atomic Absorption
- Atomic Emission
- Inductively Coupled Plasma (ICP)
- ICP/MS
- Atomic Fluorescence
- Chemicals and Reference Materials
- Data Handling/Chemometrics
- Gamma-Ray Spectroscopy
- Ion Mobility
- Imaging
- Infrared Spectroscopy
- Laser Spectroscopy
- LIBS
- Luminescence/Fluorescence
- Mass Spectrometry
- MRI
- Mobile Spectrometers
- Mössbauer Spectroscopy
- Near Infrared
- NMR, ESR, EPR
- Photonics and Optics
- Polarimetry
- Process spectroscopy
- Raman spectroscopy
- Sampling
- Separation Science
- Spectroradiometry
- Surface Analysis
- Terahertz Spectroscopy

- UV/Vis
- X-Ray Diffraction
- X-Ray Spectrometry
- None

Area of employment:

(please tick ONE only)

- Industry
- Independent Lab
- University/Institute
- Hospital
- Government
- Research Inst./Foundation
- Other _____

Job function: *(please tick ONE only)*

- Analyst
- Quality Control/Assurance
- Research Scientist
- Lab Manager
- University Professor
- Engineering/Design
- Manufacturing/Processing
- Teaching
- Marketing/Sales
- Other _____

Do you recommend, specify or authorise the purchase of spectroscopic instrumentation or services: Yes No

Your Personal Data (we will never pass your personal details to any third party)

John Wiley & Sons Ltd and IM Publications LLP will use the information you have provided to fulfil your request. In addition, please tick to receive the following options:

Digital options

- E-mail from Spectroscopy Europe/Asia about new content, products and services
- E-mail with information from carefully selected spectroscopy companies (your details are never disclosed)

Postal options

- Mailings with information from carefully selected spectroscopy companies (your details are never disclosed)
- Mailings from John Wiley & Sons and IM Publications

Now fax this page to +44-1243-811711, or return by mail to: *Spectroscopy Asia*, 6 Charlton Mill, Charlton, Chichester, West Sussex PO18 0HY, UK.

thermo scientific

Be Bold

We're on your side

Advancing your IC science – 45 years strong

Confidence in results in routine when you're partnered with best-in-class ion chromatography separation solutions. For 45 years, we've led the way in bringing reliable, reproducible analyses to dedicated people just like you. Your skills, combined with exceptional Thermo Scientific™ Dionex™ IC technology, make the ordinary extraordinary.

We honor your pursuit of bold new solutions and we're on your side to support your most ambitious goals now and into the future. You make all things possible—day in and day out—because you are one of the Bold Ones.

Find out more at thermofisher.com/ICBold